UNIVERSITY OF MANITOBA

EFFECT OF SECOND PHASE ON THE PROPERTIES OF Ni_3Ge

by

Archana Gupta

A thesis

submitted to the Faculty of Graduate Studies in partial

fulfillment of the requirements for the

Master of Science Degree in Mechanical Engineering.

1991

ISBN 0-315-76776-6

EFFECT OF SECOND PHASE ON THE PROPERTIES OF Ni_3Ge

BY

ARCHANA GUPTA

A thesis submitted to the Faculty of Graduate Studies of
the University of Manitoba in partial fulfillment of the requirements
of the degree of

MASTER OF SCIENCE

ACKNOWLEDGEMENT

The author is grateful to Dr.M.C.Chaturvedi for guidance and encouragement throughout the course of this work.

Thanks are due to Dr.A.K.Jena for helpful suggestions and to the technical staff, in particular, Messrs.J.VanDorp, D.Mardis, and L.Oree for their help at various stages of this work.The author also thanks Dr.L.Zhao, Mr.Y.Zheng and Mr.Z.He for the helpful discussions. Special thanks are due to Fariba Saadat, Ms Xiao Huang, and Ms Neharika Vohra for their great friendship and help during these two years.

Last but not the least, the author would like to thank her parents for their continuous support and encouragement.

ABSTRACT

In this work the aim was to see the effect of second phase on the properties of Ni_3Ge. Six alloys were studied namely Ni-20.0at%Ge, Ni-22.5at%Ge, Ni-23.5at%Ge, Ni-25.0at%Ge, Ni-27.5at%Ge, and Ni-30.0at%Ge. Firstly, all the alloys were characterised by doing microstructural analysis, chemical analysis on SEM, volume-fraction and grain size measurements on image analyser, lattice-parameter measurements by X-ray diffraction, microhardness and macrohardness measurement. Secondly, four of these alloys were chosen for mechanical testing. Compression tests were done on cylindrical samples at different temperatures from RT to 600°C. Failed/deformed samples were studied by doing fractography/optical metallography to get an idea about crack propagation.

Results indicated that different phases affect properties of Ni_3Ge differently. The presence of (Ni) phase improves the ductility of Ni_3Ge slightly but increases the strength to a large extent. Ni_5Ge_3 phase does not have much effect on the strength but increases the deformability tremendously. Crack propagation behavior gave a clue as to the observed behavior. In (Ni)+Ni_3Ge containing alloy the cracks were continuous and wide, present along the grain boundaries whereas in Ni_3Ge+Ni_5Ge_3 the cracks were diffused and mainly transgranular.

TABLE OF CONTENTS

LIST OF FIGURES

LIST OF TABLES

CHAPTER I

INTRODUCTION

While studying superalloys, researchers observed that the presence of intermetallic compounds makes the alloy stronger and that the strength goes up as the percentage of intermetallic precipitate in the alloy increases. In the case of $L1_2$ type of intermetallic anomalous behavior was observed. This inculcated interest to study these compounds separately as their properties suggested possible use for high temperature applications. Also, in some cases they have additional advantages over superalloys such as higher melting point and lower density.

One of the major drawbacks of intermetallics is their extremely low ductility and this is the major area of investigation. Until now, researchers have been mostly working on Ni_3Al and Ti_3Al because of their extremely low density compared to superalloys. A major success has been acheived in improving the ductility of Ni_3Al but properties like creep resistance have to be improved before their practical application is feasible.

Work on Ni_3Ge has started in recent years. Its density is almost comparable to superalloys but it shows a higher strength compared to other Ni_3X intermetallics and superalloys. However, it has a very low grain boundary cohesivity which leads to extreme brittleness. Researchers tried to improve its ductility working along similar lines as Ni_3Al but B addition to Ni_3Ge has the least effect in improving its ductility compared to other Ni_3X compounds. Other ways have been proposed to improve its ductility like microalloying, macroalloying, grain refinement, and adding a second phase. Besides these factors, a major controlling factor of ductility is the processing technique.

In this dissertation the aim was to see the effect of second phase on the properties of Ni_3Ge. Six different compositions were studied which consisted of (Ni), Ni_3Ge, and Ni_5Ge_3. After characterisation of all the samples, mechanical testing was done to see the effect of various microstructures on the properties. It was seen that the second phase alters the properties of Ni_3Ge to a large extent. Fractography was done to see the failure behavior of the compounds under different temperatures. Some reasons have been proposed as to the observed behavior.

CHAPTER II

LITERATURE REVIEW

HIGH TEMPERATURE STRUCTURAL MATERIALS

2.1 INTRODUCTION

There has been an increasing demand over the years for materials which have good strength, good corrosion/oxidation resistance, good creep resistance and other desirable properties at high temperature. Various materials such as ceramics, composites, superalloys, intermetallics, refractories etc. have been found to meet many of these requirements, but except superalloys none have yet been able to find widespread use because of certain drawbacks. Unless their properties are improved their practical applications will be limited.

Development of refractory metals started in the 1950s but poor high temperature oxidation resistance hampered their progress. Renewed interest in these materials has surfaced in recent years, but high temperature oxidation still presents a major challenge for the development of these metals for use as high temperature structural materials.

A number of oxide dispersion strengthened (ODS) alloys were introduced in the 1970s for use in the high temperature stages of gas turbine engines. In these alloys, oxide particles give superior high temperature strength but also limit their ductility. As a result, at low temperatures these alloys are quiet brittle and thus their use is presently limited to high temperature applications.

Ceramics have a number of attractive properties such as low density, high

compressive strength, high hardness and resistance to abrasion, chemical inertness, and excellent electrical and thermal insulation, which suggest that they should be ideal candidates for high temperature applications. However, they are extremely brittle in tension and very difficult to process and hence their use as structural materials won't be realized until their toughness is improved.

Composites are the most recent development in the area of high temperature structural materials and the properties of both metal-matrix composites and intermetallic-matrix composites can be tailored to meet the requirements of the particular application. In these, usually the properties of one constituent enhances the limiting properties of the other (e.g stiff SiC fibers in a softer aluminum matrix or ductile niobium fibers in a brittle TiAl intermetallic matrix.).

Superalloys and intermetallic compounds are discussed in greater detail in the following chapters.

2.2 SUPERALLOYS

Development of superalloys began in the 1930s as a result of the need for better heat resistant materials. They offer an attractive range of properties needed for high temperature use. According to the American Society for Metals(1) definition:

" A superalloy is an alloy developed for elevated temperature service, usually based on group VIIIA elements, where relatively severe mechanical stressing is encountered and where high surface stability is frequently required."

The superalloys have been classified into three major classes: cobalt base, nickel base, and iron base. Their present day applications range from aircraft, marine, industrial and vehicular gas turbines to space vehicles, rocket engines, experimental aircraft, nuclear reactors, submarines, steam power plant, petrochemical equipment, and other high temperature applications. However, their major use is in the gas turbine industry[1].

2.2.1 MECHANICAL PROPERTIES

Superalloys consist of a number of alloying elements which produce a combination of high strength at elevated temperatures, resistance to creep at temperatures upto 1000°C, and resistance to corrosion. To obtain high strengths, the alloying elements must produce a strong stable microstructure at high temperatures.

Some of the major properties of superalloys are outlined below:

- high temperature strength

- good ductility

- outstanding impact resistance and good resistance to high cycle and low cycle mechanical fatigue as well as thermal fatigue

- densities in the range of 0.28 to 0.335lbs/in^3

- low thermal conductivity

- oxidation resistance: minor additions of active elements such as yttrium, lanthanum, or cerium promote scale retention and improve oxidation resistance

- hot corrosion: it is related to the chromium content in both nickel and cobalt base alloys and is also a function of the sulfide properties of these systems.

Phase instability in superalloys enables their properties to be varied by different heat treatments.

2.2.2 HARDENING MECHANISMS

Hardening can be acheived in superalloys by alloying additions which can be either through solid solution strengthening or precipitation strengthening. Precipitation strengthening can occur due to formation of gamma prime phases, carbides, or borides[1].

This will be discussed in detail in section 2.3 on Ni-base superalloys.

2.2.3 PROCESSING TECHNIQUES

As new processing techniques developed it became evident that processing was one of the major factors governing the properties of superalloys. Thus, it helped in understanding the way in which inclusions, grain size, and grain boundaries affect the

mechanical properties of superalloys.

(1) Vacuum melting (1950): this removes oxygen and nitrogen from the melt and prevents the formation of unwanted oxide and nitride inclusions.

(2) Investment casting (1956): alloys offer superior rupture strength over wrought alloys because casting leads to increased grain sizes and beneficial segregation in the casting.

(3) Dispersion strengthening (1962): the formation of a fine dispersion of oxide particles through powder metallurgy techniques leads to exceptional high temperature strengths for some nickel alloys.

(4) Directional solidification (1967): controlling grain orientation by directional solidification techniques greatly improves resistance to intergranular fracture at high temperatures in the direction of applied stress.

(5) Single crystal casting (1968): the removal of grain boundaries by the growth of single crystals eliminates grain boundary failures in the alloys.

By incorporating this knowledge into their processing procedures, people have been able to significantly increase the high temperature strength of nickel base alloys.

2.3 Ni-BASE SUPERALLOYS

These are the most complex of all superalloys and their use extends to the highest homologous temperatures of any common alloy system. They are the most widely used for the hottest parts and currently comprise over 50% of the weight of advanced aircraft engines[1]. Heat resistant Ni-alloys are frequently used for furnace parts and other heat treating equipment. Nuclear power plant applications include steam generator tubing and

structural components of reactor cores. As a class, nickel base superalloys exceed stainless steels in mechanical strength especially at high temperatures (>650°C)[2].

Research in the past forty to fifty years has advanced nickel base superalloys to this remarkable level of engineering utility. There is no other alloy class offering the total balance of engineering properties in polycrystalline form and there is no other structural material which offers a service temperature at as high a fraction of its melting point as the superalloys do in single crystal form.

To surpass the nickel base superalloys, materials to be developed should have either low density or higher melting point.

Most of the nickel alloys contain 10-20% chromium, upto about 8% aluminum and titanium, and small amounts of boron, zirconium, and carbon[1]. Ni-base heat resistant alloys contain 30 to 75% nickel and up to 30% chromium. Many Ni-base alloys contain small amounts of Al, Ti, Nb, Mo, and W to enhance either strength or corrosion resistance[2].

There are three major classes of elements that help in giving the required strength and structure to nickel base superalloys[1]. The first class consists of elements from group V, VI, and VII which make up the FCC austenite matrix e.g Ni, Co, Fe, Cr, Mo, W, and V. The second class consists of elements from group III, IV, and V which make the gamma prime precipitate Ni_3Al and the third class of elements that segregate to grain boundaries which include Mg, B, C, and Zr from groups II, III, and IV. Within these major classifications there are two subclassifications. One includes carbide formers: Cr, Mo, W, V, Cm, Ta, and Ti. The second subclass comprises oxide formers, chromium and

aluminum, which develop adherent diffusion-resistant oxides to protect the alloys from the environment.

The major phases present in the nickel base alloys are the FCC austenite (γ, the matrix of the alloys), gamma prime (γ', the major precipitate phase), and carbides. In addition to these, the alloys may have grain boundary gamma prime and topologically close packed (TCP) type phase. Following is a brief description of the way in which each of these help in hardening the alloy.

2.3.1 SOLID-SOLUTION STRENGTHENING

Solid-solution elements in γ are usually cobalt, iron, chromium, molybdenum, tungsten, vanadium, titanium, and aluminum. All these elements differ from nickel by 1-13% in atomic diameter. Thus, strengthening can be attributed to the lattice parameter mismatch between solvent and solute. Fleischer suggested[1] that modulus differences between solute and solvent may give rise to strengthening because extra work is needed to force a dislocation through hard and soft regions in the matrix. Fig 2.1 demonstrates the effect of lattice parameter change on the flow stress for different solute elements[1].

2.3.2 GAMMA PRIME PHASES(γ')

A high nickel matrix favors the precipitation of γ', which requires little size change. The low mismatch of γ' fcc crystal with γ results in homogeneous nucleation of a precipitate with low surface energy and extraordinary long time stability.

γ' is an A_3B type of compound where A is composed of relatively electronegative elements such as nickel, cobalt, or iron and B is composed of electropositive elements

such as aluminum, titanium, or columbium.

γ' contributes strengthening to the γ-γ' alloy since it poses barriers for dislocation motion and hence contributes antiphase boundary strengthening . It is seen from fig 2.2 that as the percentage of γ' increases, the yield stress versus temperature behavior of the material changes from regular to anomalous behavior. This has been observed in the case of $L1_2$ type of A_3B compounds like Ni_3Al and is discussed in detail later.

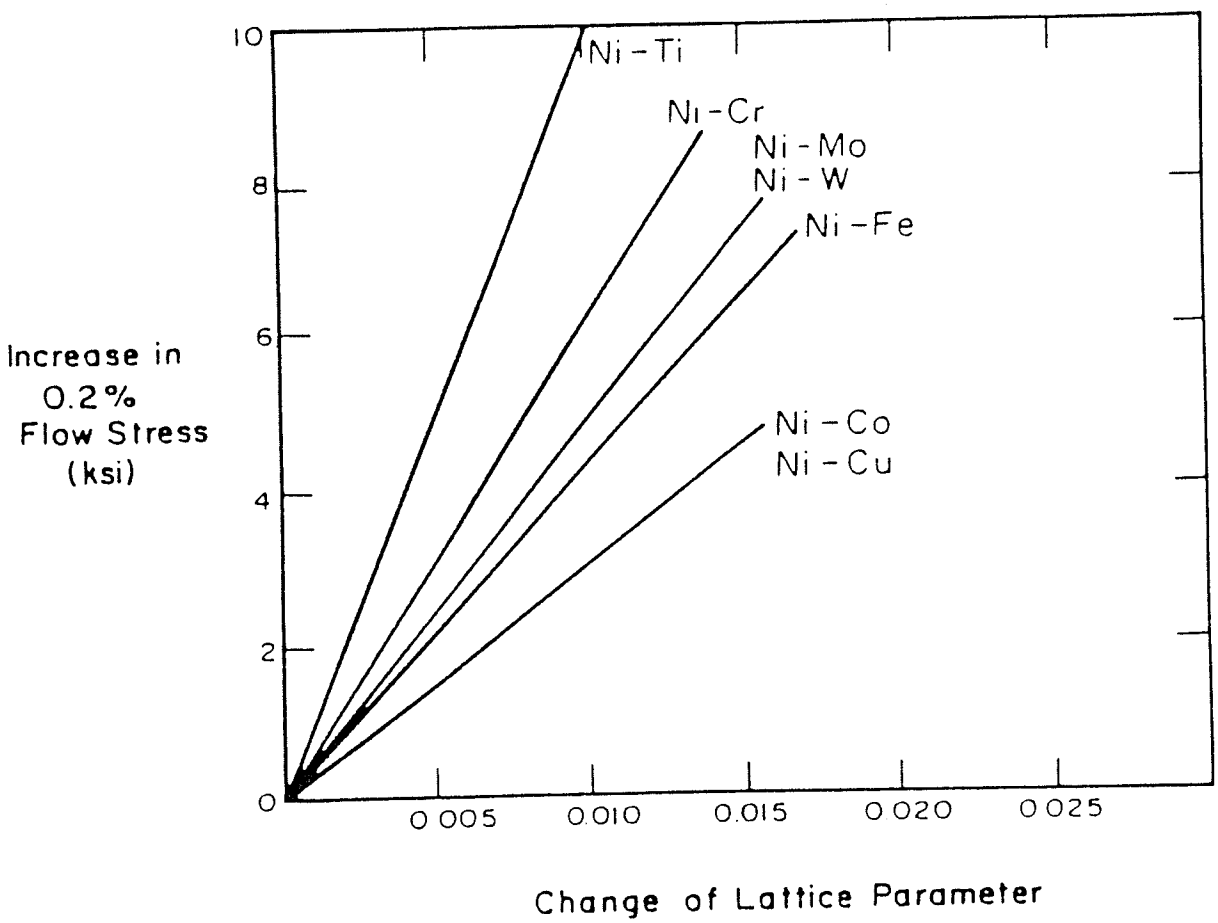

Fig 2.1 Effect of lattice parameter on flow stress of nickel alloys[1]

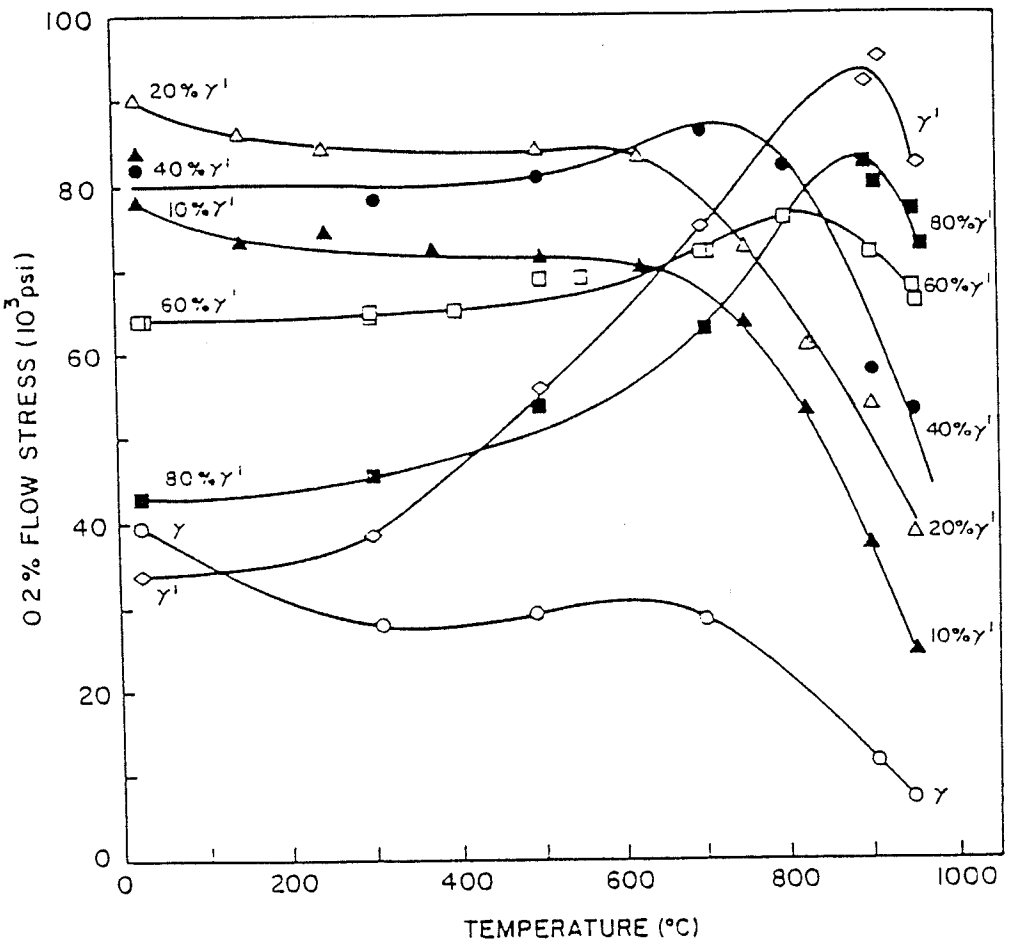

Fig 2.2 Flow stress of polycrystalline Ni-Al-Cr alloy as a function of temperature for different volume fraction of gamma prime [γ'][8].

Other possible factors governing the hardening of austenite superalloys by coherent particles are as follows[1]:

(1) coherency

(2) differences in elastic moduli between particle and matrix.

(3) existence of order in the particles.

(4) differences in SFE of particle and matrix

(5) energy to create additional particle -matrix interface.

(6) increases in lattice resistance of particles with temperature.

The shape of γ' is dependent upon the matrix-lattice mismatch. It is spherical for 0-0.2% lattice mismatch, cubic for 0.5-1.0%, and platelike at mismatches above 1.25%.

2.3.3 CARBIDES

Carbides in superalloys play a complex and dynamic role. They can occur at the grain boundaries or intragranular sites and their morphology affects ductility and also chemical stability of the matrix through removal of reacting elements.

The common classes of carbides are MC, $M_{23}C_6$, Cr_7C_3, and M_6C. $M_{23}C_6$ carbides have a significant effect on alloy properties because of their presence at grain boundaries which inhibits grain boundary sliding and thus affects rupture strength. M_6C carbides are stable at high temperatures and thus are beneficial as a grain boundary precipitate to control grain size in wrought alloys.

2.3.4 BORIDES

Boron is an essential ingredient in superalloys. It occurs at grain boundaries where, at the intersecting structure, it reduces the onset of grain boundary tearing under rupture loading. Borides are hard, refractory particles observed only at the grain boundaries. Their shapes range from blocky to half moon in appearance.

2.3.5 TOPOLOGICALLY CLOSE PACKED (TCP) PHASES

In certain alloys where composition has not been carefully controlled, undesirable hard phases can form during heat treatment. TCP phases[1] are characterised as comprising of close-packed layers of atoms forming in Kagome (basket weave) nets aligned with the octahedral planes of the FCC matrix. These, generally detrimental, phases appear as thin plates, often nucleating on grain boundary carbides. Those commonly found in nickel alloys are σ,μ, and laves[1].

2.4 INTERMETALLIC COMPOUNDS

Intermetallic compounds can be defined as intermetallic phases exhibiting long-range order over the entire temperature range of stability[3]. These phases usually occur at a definite atomic ratio and most often exhibit a narrow homogeneity range. The homogeneity range may result by the formation of vacancies or by the formation of a slightly random solid solution. Both of these mechanisms may also result in nonstoichiometric compounds; i.e. compounds whose temperature range of stability does not include the composition corresponding to the fully ordered structure. Non-stoichiometry in ordered intermetallics is a very important crystallographic parameter affecting their physical and mechanical properties. These compounds occupy an intermediate position between metallic alloys based on solid solutions or solid solutions with second phase strengtheners on one extreme and ceramics on the other.

Ordered intermetallic alloys are among the most promising class of materials being developed for future high temperature applications. They have crystal structures that are more complex than those of ordinary metals. The existence of atomic ordering leads to fundamental changes in the microscopic behavior of these alloys and these changes in microscopic behavior in turn leads to the unique macroscopic properties that makes intermetallic alloys attractive for high temperature use.

Thermodynamic properties of intermetallic compounds can attribute to an understanding of their nature. A decrease in free energy accompanies the formation of an intermetallic compound from its component elements. A compound is stable with respect

to competing neighbouring phases in a multicomponent system if its free energy is lower than that of a mixture of these phases. The minimum value of the free energy of intermetallic compound existing over a homogeneity range has often been assumed to occur at the stoichiometric composition on which such a compound appears to be based.

In general, intermetallic compounds have higher melting temperatures and lower densities than Ni-base superalloys, and are considered ideal candidates for further development as high temperature materials[4].

These compounds occur in a variety of crystal structures. The four most common type of solid solutions in which the formation of a superlattice does not change the crystal structure, but only lowers the symmetry are shown in fig 2.3 and examples of each of these types are listed in table 2.1[5].

Intermetallic compounds have properties which make them extremely interesting from both a scientific and technological viewpoint[3]. They are scientifically interesting because they provide a whole range of phenomena which are not seen in disordered alloys, but against which the applicability of classical theories of strengthening, deformation, and fracture can be tested. They are interesting from a technological point of view because they tend to be strong and rigid. Some of the major properties of intermetallics are:

- high temperature strength
- high melting point
- low density
- good corrosion/oxidation resistance

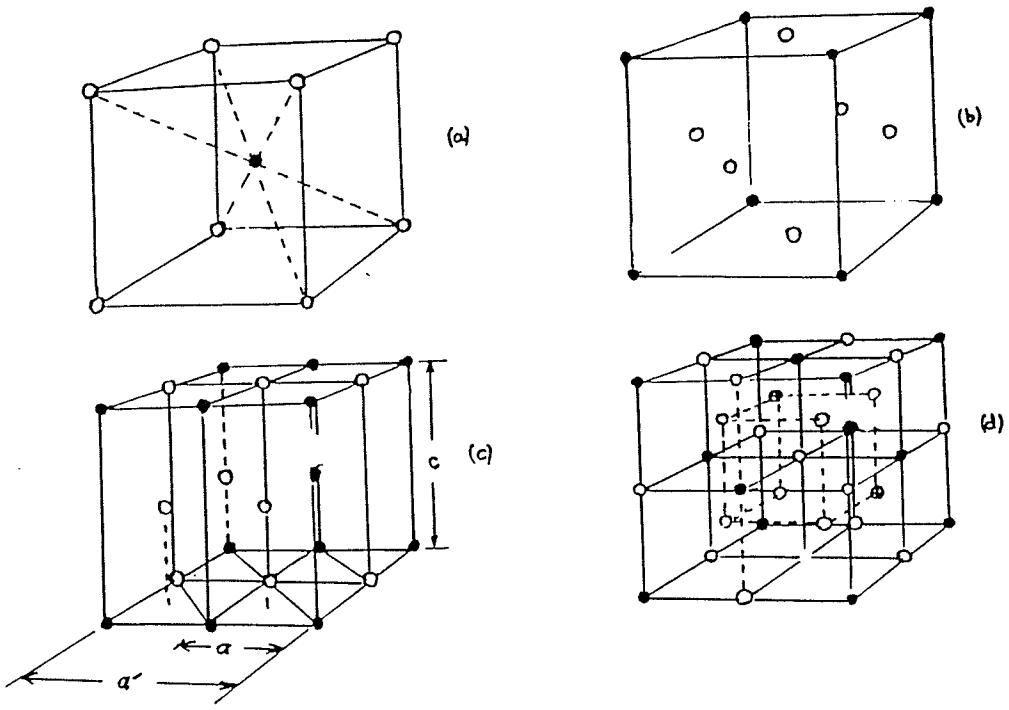

Fig 2.3 Common types of superlattices (a) $L2_0$, (b) $L1_2$, (c) DO_{19}, (d) DO_3[5]

Structure type	Examples
$L2_0$	CuZn, FeCo, NiAl, CoAl, FeAl AgMg
$L1_2$	Cu_3Au, Au_3Cu, Ni_3Mn, Ni_3Fe, Ni_3Al, Pt_3Fe, Ni_3Ge
DO_{19}	Mg_3Cd, Cd_3Mg, Ti_3Al, Ni_3Sn
DO_3	Fe_3Al, Fe_3Si, Fe_3Be, Cu_3Al
$L1_0$	AuCu, CoPt, FePt, FePd

Table 2.1 Examples of the various structure types[5]

- good creep resistance

Thus, there are several reasons as to why ordered intermetallics are intrinsically more appealing than disordered compounds. Most importantly, they tend to be very strong (high yield or fracture stress) and the strength tends to be maintained at high temperatures. Others having $L1_2$ type of structure show anomalous behavior. For normal metals and alloys it is seen that the strength decreases as the temperature increases but in case of some $L1_2$ type of intermetallics it is observed that the strength exhibits a maximum at elevated temperature (fig 2.4).

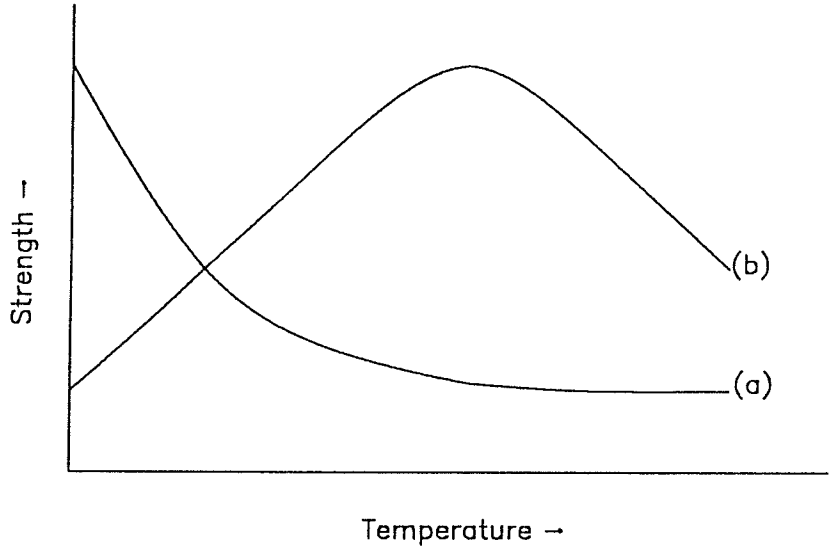

Fig 2.4 Schematic drawing showing variation of yield strength with temperature for (a) general metals and alloys (b) $L1_2$ type intermetallic compounds

This property is particularly useful for high temperature applications. Not only is the strength of intermetallics maintained to high temperatures, the modulus tends to be high and tends to decrease more slowly with increasing temperatures than does that of disordered alloys. Some of these compounds such as Ti_3Al can have extremely low

densities. Thus, the low density combined with the high strength and modulus gives rise to very attractive specific properties which are especially important for rotating machinery and aerospace applications.

A better creep resistance is obtained because of the ordered structures which make it difficult for the solute atoms to diffuse thus resulting in lower diffusion rates.

But unfortunately, despite having all these attractive properties, they have a major drawback and that is their extremely low ductility especially at low temperatures. In fact, a loss of ductility is commonly the first indication of the occurence of an intermetallic compound in an alloy. Commonly, the crystal structures of intermetallics have large unit cells and complex constructions compared with usual metals and alloys, resulting in a higher peierls stress and lack of operative slip systems. Therefore, it has been considered basically impossible to expect the deformability of intermetallic compounds[6]. The ductility problem is a particularly important one because the development of future high temperature alloys with better high temperatures properties than modern Ni-base superalloys almost certainly will involve the use of intermetallics with complex atomic structures. These intermetallics will probably have very low ductility at low temperatures. Thus, research must be directed towards improving the ductility of these complex intermetallics.

The brittleness results for two reasons[6]:

(1) an insufficient number of slip systems

(2) grain boundary weakness

In the case of complex intermetallics, the number of slip systems operating is very

low and hence the resulting brittleness. However, for $L1_2$ type intermetallics, more than five slip systems are operative and hence the brittleness cannot be attributed to the first factor. Also, for some $L1_2$ type compounds, it has been shown that single crystals of these materials are not brittle. This implies that for $L1_2$ type compounds the brittleness can wholly be attributed to the second cause; i.e. grain boundary weakness.

This grain boundary weakness might be a result of either intrinsic factors or extrinsic factors. Extrinsic factor results due to segregation of harmful impurities at the grain boundary area such as sulfides. Intrinsic factor may result due to poor cohesive strength of the grain boundary or due to the difficulty of slip being transmitted across grain boundaries leading to stress concentrations which are relieved by cracking. Grain boundary cohesivity depends on three factors: valency difference between A & B atoms, size difference between A & B, and electronegativity difference between A & B. Grain boundary brittleness may also be due to higher grain boundary energy, which includes not only normal grain boundary energy, as in other disordered metals and alloys, but also antiphase boundary energy due to long range ordered structure. It is believed that the higher the grain boundary energy, the less stable the grain boundary, i.e it is easier for it to undergo decohesion and that the segregation of harmful impurities at the grain boundary area may aggravate the brittleness because of its influence on the grain boundary energy.

Researchers have been working mainly on Ni_3Al and Ti_3Al. After trying various methods they have proposed certain ways to improve the ductility & strength, some of which are listed below:

(1) Microalloying : This is done to improve the ductility and can be done by adding two types of elements. First, reactive elements which can combine with the impurities and thus get rid of the extrinsic factor for grain boundary brittleness.e.g Mn, Mg, Ca, Ce etc. Second are those elements which act as electron donors to increase the cohesive strength of the boundaries e.g C, B, Be etc.[58]

(2) Macroalloying or solid solution hardening: Similar to general metals and alloys, alloying is an important way to improve the strength and other mechanical properties of intermetallic compounds. These ternary additions are mainly the A-subgroup elements and transition metal elements.The addition of ternary elements has been found not only to increase the flow stress but to also increase the rate of increase of flow stress with temperature; i.e alloying usually lowers the peak yield strength temperature e.g Hf, Zr, Ta etc.[58]

(3) Introducing a second phase : The strength of single phase alloyed gamma prime is considerably lower than that of an advanced two-phase Ni-base superalloys. The reason for this may be because in single phase alloyed Ni_3X, dislocations generate in a continuous Ni_3X solid solution, and during the motion of the dislocations there is no increment of antiphase boundaries although there exists antiphase boundaries between dislocation pairs. Therefore, the strength of single phase Ni_3X cannot be expected to be very high, and second phase strengthening should be considered in developing Ni_3X base superalloys.Second phase can be introduced by two methods; first is by changing the composition either towards the A-rich or B-rich side in the A_3B type of compound.Second by adding carbon to precipitate carbides[8].

Huang and Hall[7] found that a duplex structure which contains both primary γ grains and transformed γ/α_2 lamellar grains is more deformable than a single phase or fully transformed structure. They said that the deformation of these duplex alloys is facilitated by 1/2[110] slip and {111} twinning but very limited superdislocation slip occurs. The twin deformation is suggested to result from a lowered stacking fault energy due to oxygen depletion or an intrinsic change in chemical bonding. Other factors such as grain size, grain boundary chemistry and structure are important from a fracture point of view.

(4) Grain refinement: This can be done either by heat treatment after a certain amount of deformation or by adding certain elements. Researchers do not agree on the issue whether grain size has any effect on the strength or not and work is still going to confirm the exact affect of grain size on strength.

2.5 Ni_3Al

Development of Ni-base superalloys has been in progress for the last fifty years and their temperature capability has increased a lot in these years. This success has been attributed mainly to the presence of coherent ordered FCC $Ni_3Al(\gamma')$ particle as the main strengthening phase of the matrix. The strength and operating temperatures of these alloys increase with increasing volume fraction of γ' phase. With increasing volume fraction of γ' the operating temperature of Ni-base superalloys has reached to 0.85 to 0.90Tm. Therefore, the development of Ni_3Al base superalloys is necessary to extend the upper temperature limit[1].

Some of the properties of Ni_3Al are:

- It has an $L1_2$ ordered FCC crystal structure and has five independent slip systems which is an essential condition for ductility.
- High M.P(1385°C) than all commercial Ni-base alloys.
- Good oxidation resistance (due to the formation of protective Al_2O_3 film).
- low density.
- Very good castability and has a relatively low material cost.

But as discussed earlier the brittleness of intermetallic restricts it's application. The reasons for brittleness are the same as discussed in the previous section on intermetallics. In the following section a brief review of the work done on Ni_3Al is presented.

2.5.1 REASONS FOR BRITTLENESS

In the case of Ni_3Al it has been found that sulfur is a trace element that strongly segregates to the grain boundary and may embrittle the boundaries [8,9,10].

Electronic and structural studies of grain boundaries of binary A_3B alloys show that most of the atomic bonds in the grain boundary areas of Ni_3Al are Ni-Ni bonds and the bonding energy of these bonds is lower than that of Ni-Al bonds i.e, H_{Ni-Ni}=-71.33KJ/g.atom, H_{Ni-Al}=-74.08KJ/g.atom. Therefore, the strength of the grain boundary is lower than that of the grain interior[11]. For microalloying, various elements have been tried including B, C, Be, Ti, Ce, Ca, Mg, Mn, and Si. Among these B has been found to be the most effective element in improving the ductility and fabricability of polycrystalline Ni_3Al.

2.5.2 EFFECT OF BORON

Aoki and Izumi[12] first discovered the beneficial effect of boron in Ni_3Al. Liu and coworkers[13] were able to enhance the tensile elongation of polycrystalline Ni_3Al to over 50% by a careful control of bulk boron content, alloy stoichiometry, and thermomechanical treatment. It was observed that the addition of boron results in a change in fracture morphology from primarily intergranular to largely transgranular.

Fig 2.5 shows the effect of boron addition on room temperature tensile properties. The figure shows that there is a sharp increase in ductility from near 0 to 44% as the boron content is increased from 0 to 0.025%. The ductility increases to 54% at 0.1%boron but on further increases in boron content, the ductility goes down. It has been shown that

the optimum concentrations of boron which show the highest elongation differ due to difference in grain sizes. The smaller the grain size, the higher the value of the optimum B content since the material with smaller grain size contains more grain boundary area and hence needs more boron.

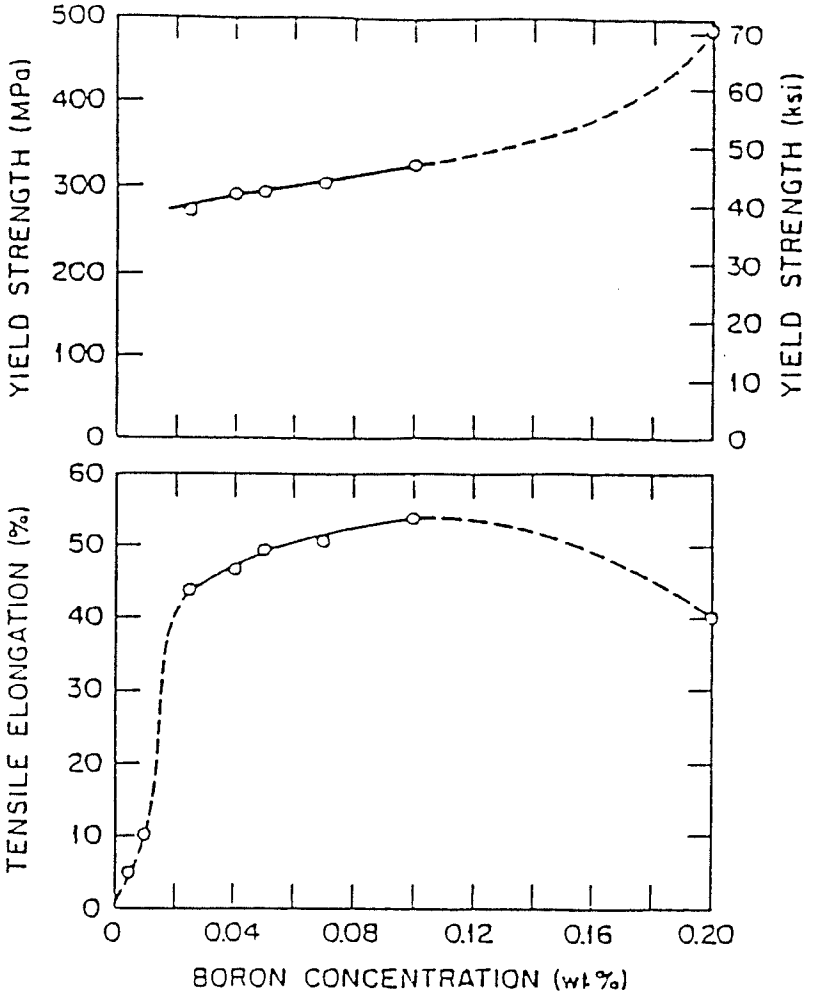

Fig 2.5 Plot of RT tensile properties as a function of boron concentration for Ni_3Al[13].

Although the addition of B can improve the RT ductility and yield strength significantly, the improvement of high temperature yield strength due to the addition of boron has been found to be very limited as shown in fig 2.6[19].

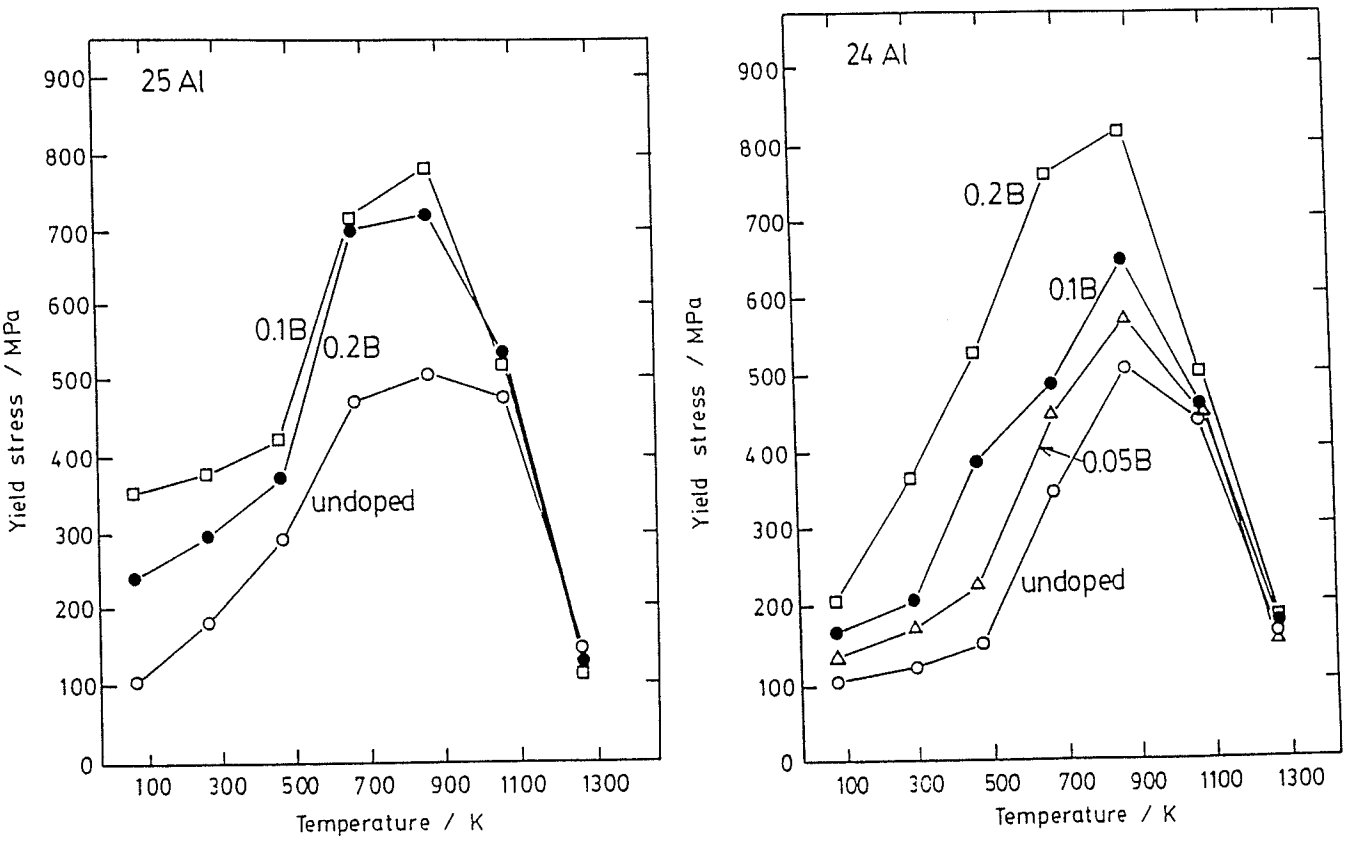

Fig 2.6 Temperature dependence of the yield stress for B-doped Ni_3Al alloys

(a) B-doped 75Ni-25Al alloys (b) B-doped 76Ni-24Al alloys[19].

Following are the mechanisms proposed to explain the benefit of boron addition in polycrystalline Ni_3Al:

(1) Messner and Briant[14] proposed an electronic model to explain the effects of alloying elements on the grain boundary cohesion in metals. Boron acts as a beneficial or cohesion enhancing element, does not draw charge out of the base metal atoms and thus does not weaken the metal-metal bonds. Boron has an electron configuration of $1s^2 2s^2 p^1$ and is therefore not a sink for electrons. It can however share or contribute the p electron, forming homopolar bonds, and therefore enhance bonding of the grain boundaries.

(2) This model is based on B-induced disordering in the grain boundary area. This model suggests that B segregation disorders the grain boundary region so that stresses due to dislocation pileups can be relieved by slip transmittal across the grain boundary rather than by cracking[15,16,17].

(3) Studies have shown that addition of boron changes the microstructure of the alloys. When the boron content exceeds 0.5at%, small angle grain boundaries appear which make the slip across the grain boundary easy and decreases the stress concentration at the boundaries[18].

It has been found that both C and Be additons can also strengthen Ni_3Al in the temperature range of 77K to 1100K. The addition of Be(upto 0.2wt%) can improve the ductility of Ni_3Al upto 5% whereas addition of C does not improve the ductility and has little effect in improving the ductility of polycrystalline Ni_3Al[19].

2.5.3 SOLID SOLUTION HARDENING OF NI_3AL BY TERNARY ADDITIONS

A-subgroup elements and transition metal elements have been employed as alloying additions to improve the strength and other mechanical properties of Ni_3Al. It has been found that Hf, Zr, and Ta are the most beneficial elements in strengthening Ni_3Al at room temperature or at elevated temperatures.

Recently, Mishima, Ochiai, Yodogawa, and Suzuki[20,21,22] systematically studied the effects of the A-subgroup elements(Si, Ge, Ga, In, Sn,Sb) and transition metal elements (Ti, Zr, Hf, V, Nb, Ta, Mo, W) on the tensile yield strength of polycrystalline Ni_3Al in the temperature range of 77K to 1173K. Their results show that the addition of all these elements improves the yield strength in this temperature range. Typical curves reflecting the temperature dependence of 0.2% flow stress of Si and Hf containing Ni_3Al are shown in fig 2.7. It is seen that the addition of Hf is more effective than Si. The variation in the relationship of yield stresses at 77K and peak yield stresses with ternary solute concentrations in Ni_3Al with addition of different elements are shown in fig 2.8 & 2.9.

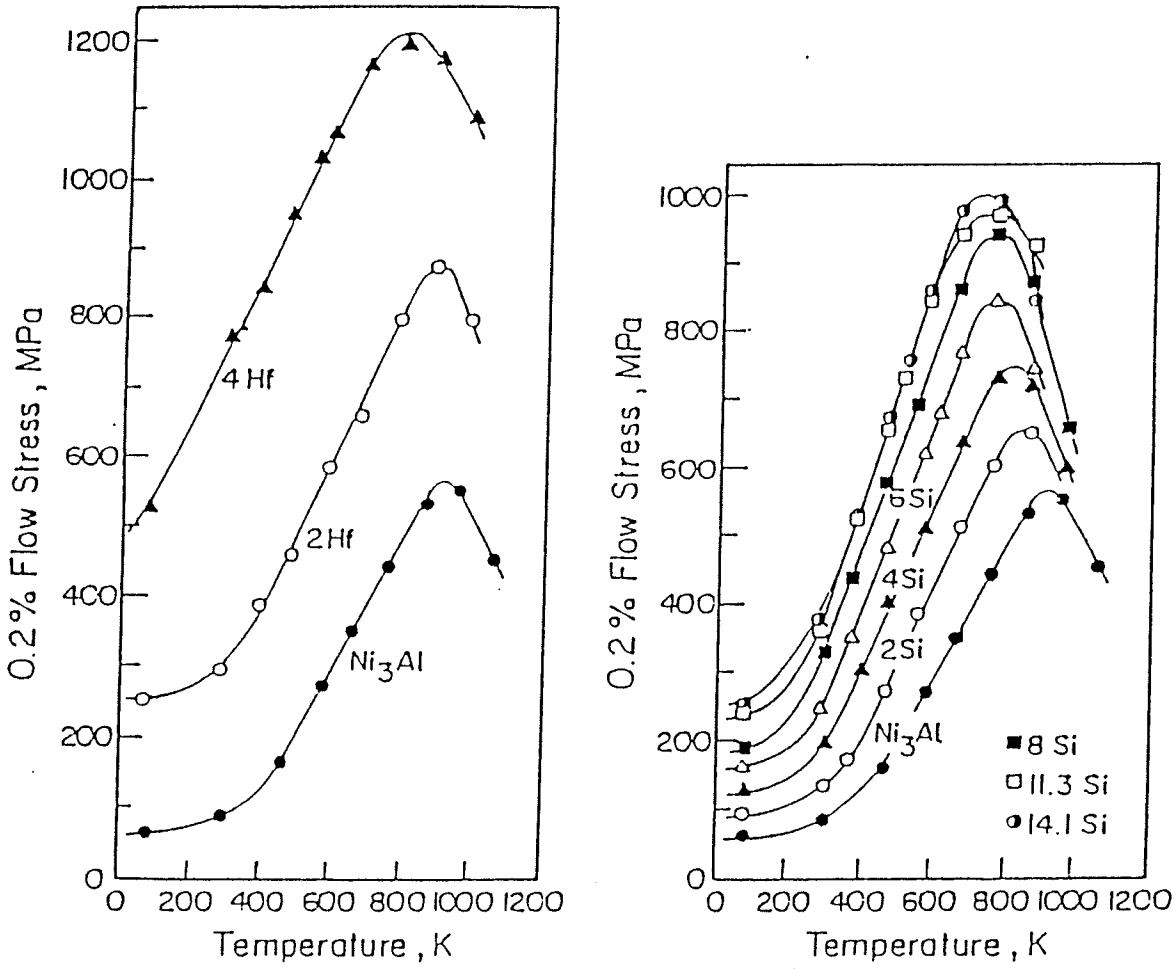

Fig 2.7 Temperature dependence of 0.2%flow stress in Ni_3Al with addition of Hf and Si[20].

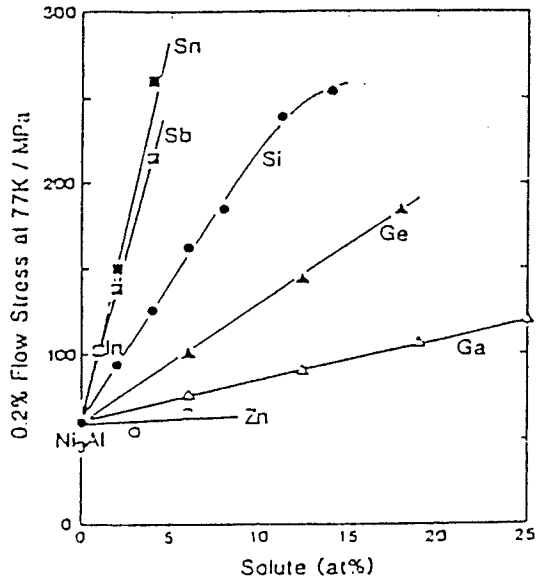

Fig 2.8 Relation between 0.2% flow stress measured at 77K and solute concentration in ternary Ni_3Al with addition of A-subgroup elements[20].

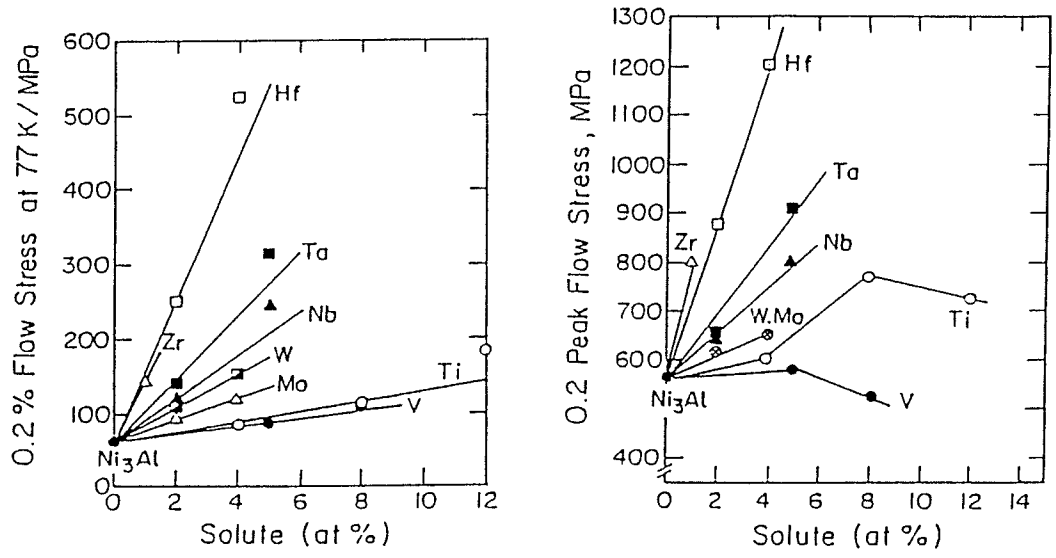

Fig 2.9 Relation between 0.2% flow stresses and the solute concentration in ternary Ni_3Al with addition of transition metal elements[21].

The addition of ternary elements in Ni_3Al not only increases the flow stress but also increases the rate of increase of flow stress with temperature, i.e alloying usually lowers the peak yield strength temperature.

2.5.4 DEVELOPMENT OF TWO PHASE NI_3AL BASE SUPERALLOYS

In Ni_3Al base alloys, the second phases can be introduced by two methods. One is by adjusting the ratio of Ni/Al. Ni(or plus elements substituting for Ni)-rich contents can produce (γ+γ') Ni_3Al base alloys, and in Al (or plus elements substituting for Al)-rich systems, β(NiAl) phase with precipitate in γ' matrix to form γ'+β Ni_3Al base alloys. Another way to introduce a second phase in Ni_3Al is by adding some special alloying elements to form carbides and/or borides.

2.6 Ni_3Ge

2.6.1 INTRODUCTION

Ni_3Ge is an ordered intermetallic compound having $L1_2$ type of structure. It occurs in the range of 22.5 to 25 at% Ge in the phase diagram. It's properties are similar to Ni_3Al in many respects. It also shows good high temperature strength and exhibits anomalous behavior. However, as in case of other intermetallics it has a major drawback which is it's extreme brittleness. Since considerable success has been acheived in improving the ductility of Ni_3Al by boron addition, work along similar lines is progressing to improve the properties of Ni_3Ge.

Ni_3Ge alloys consist of large columnar grains[23]. Ni_3X compounds are brittle inspite of pure nickel being ductile because pure nickel has completely metallic bonding in which the electrons should be able to adjust their positions to provide bonds across a structural imperfection such as a grain boundary. However, once elements such as Al, Ga, Si or Ge are added to the point that ordering can occur, it is quiet possible that a madelung type component will enter the description of the bond. In this situation, some of the electronic charge would be localised between the atoms and less electronic charge would be available to participate in the A-A bonds that hold the boundary together[24].

2.6.2 REASONS FOR GRAIN BOUNDARY FRAGILITY IN Ni_3Ge

As discussed in a previous section, the grain boundary fragility of intermetallics is a major hindrance to their development. Out of all the Ni_3X alloys like Ni_3Al, Ni_3Ga,

Ni_3Si, and Ni_3Ge ductility results indicate that the grain boundary strength of Ni_3Ge is the weakest. In order to improve the ductility, the reasons for this brittleness must first be understood.

Here only the intrinsic factors associated with the brittleness of Ni_3Ge are discussed. As discussed previously, low grain boundary strength can be explained on the basis of valency difference between A and B atoms, size difference between A and B atoms, and electronegativity difference between A and B. Takasugi and Izumi's[23] results suggest that the degree of the intergranular strength and related failure behavior primarily depend upon the electronic chemical bonding nature between the A and B atoms. They showed that compounds with a larger valency difference between the two atoms are more prone to intergranular fracture (Table 2.2). They further postulate that the cohesive strengths can be further differentiated by size effects. As the size difference increases, the cohesive strength of the boundary should decrease[24].

To determine the size effects, two parameters can be used namely lattice parameter of the Ni_3X alloys which can be compared with that of pure nickel and the lattice strains observed for solid solutions of the various X species in FCC nickel. If one combines the valency and size difference effects, one finds that the model predicts the cohesive strengths for the Ni_3X alloys of interest to vary such that $Ni_3Fe > Ni_3Mn > Ni_3Al > Ni_3Ga > Ni_3Si > Ni_3Ge$. Without boron doping, the latter four compounds exhibit brittle intergranular fracture so the cohesive strengths cannot be ranked. With boron doping, only Ni_3Ge was not made ductile. If it is assumed that the boron provides additional cohesive strength to the grain boundary and that this additional increment of strength is

superimposed on the inherent strength of the boundary in the binary compound, then the ductility results indicate that the grain boundary strength of the germanium compounds are the weakest of the four alloys studied[24].

Electronegativity differences between the two atoms can also be used to explain the grain boundary fragility. In A_3B compounds, geometric modelling has shown that the A-A bonds dominate at the grain boundary (fig 2.10), therefore the cohesive strengths could be determined by the extent to which the B atom pulls the electronic charge out of these A-A bonds. The electronegativity model predicts that the grain boundary cohesive strength of the Ni_3X intermetallics will decrease when the electronegativity of the X-species becomes greater than that of Ni resulting in charge transfer away from Ni-Ni bonds[25]. From the table we see that since Ge is the most electronegative of the atoms listed it is therefore most likely to draw charge out of the Ni-Ni bonds. Based on this argument, Ni_3Ge is expected to have the lowest cohesive strength in agreement with the ductility results.

X Species	Valency Difference	Lattice Dilation	Electroneg. Difference	Undoped Alloy	B-Doped Alloy
Fe	0.2	+1.0%	-0.08	ductile	-
Mn	0.9	+2.2%	-0.36	ductile	-
Al	3.0	+1.5%	-0.30	brittle	ductile
Ga	3.0	+1.6%	-0.10	brittle	ductile
Si	4.0	-0.04%	-0.01	brittle	ductile
Ge	4.0	+1.5%	+0.10	brittle	brittle

Table 2.2 Valency-Size Effect-Electronegativity Correlation With ductility in the $L1_2$ Ni_3X alloys.[24]

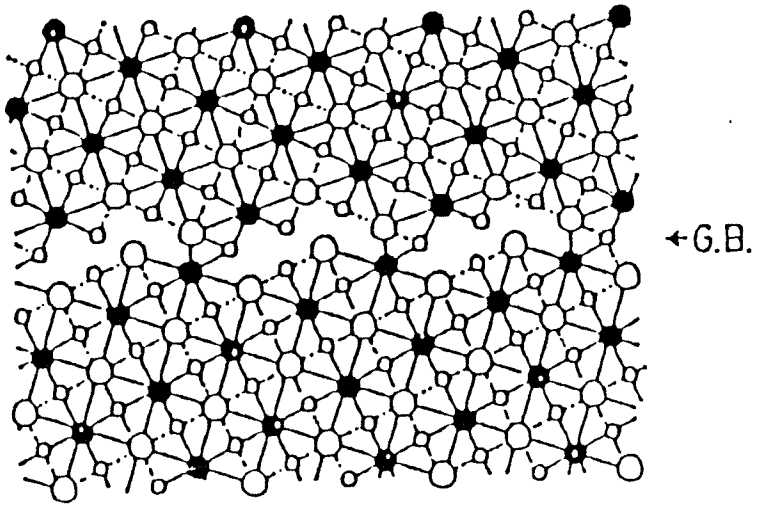

Fig 2.10 Schematic representation of the effect of covalent bonds between A & B atoms at a grain boundary of the $L1_2$ A_3B alloys[6].

2.6.3 ANOMALOUS BEHAVIOR OF ORDERED $L1_2$ INTERMETALLICS

One of the most striking features of the plastic deformation of most ordered alloys, in particular many of those having the $L1_2$ structure (e.g Ni_3Al, Ni_3Ge, Ni_3Si, Ni_3Ga, Zr_3Al) is an anomalous sharp rise in flow stress with increasing temperature (fig 2.11). The peak in flow stress occurs in single crystals as well as in polycrystals[26,36].

Liang and Pope[28] have shown that order-disorder effects play an important role in the flow stress of alloys having $T_c << T_m$ where T_c is the temperature of transition from ordered to disordered state and T_m is the melting temperature of the alloy (e.g Cu_3Au,Ni_3Fe etc) but not in the alloys having $T_c >= T_m$ (e.g Ni_3Si, Ni_3Ga, Ni_3Al, Ni_3Ge etc).

Three factors control such anomalous behavior as reported by Suzuki et al[37]

(1) Antiphase boundary (APB) energy on {111}

(2) S.F. energy

(3) APB energy on {100}

The high anisotropy of APB energy between {100} and {111} is believed to be responsible for the strength anomaly in $L1_2$ alloys because of the limited cross-slip of the leading superpartials onto {100} planes to minimize APB energy.

The positive temperature dependence of strength has been successfully explained by the Kear-Wilsdorf mechanism[41,42]; i.e.with increasing temperature the drag stress is increased by the formation of sessile segments on mobile screw dislocations.

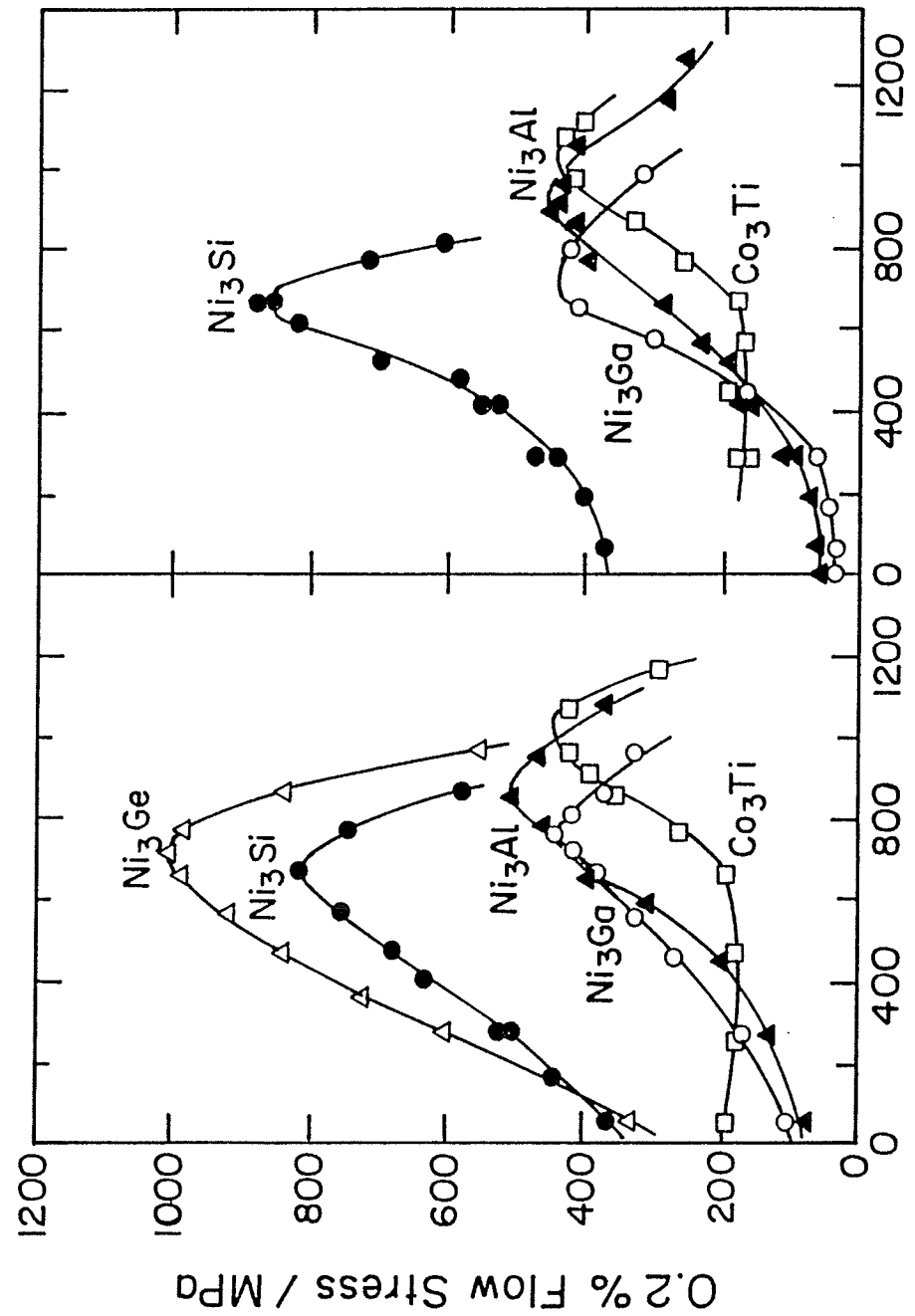

Fig 2.11 Temperature dependence of the flow stress of nickel-based $L1_2$ alloys and Co_3Ti[26]

Thermally activated cross slip from {111} to {010} planes occurs because in the $L1_2$ crystal structure the normal slip plane and the lowest antiphase boundary (APB) energy plane are not identical. This mechanism, however, does not appear to be sufficient in order to explain the different temperature response of mechanical behavior among the different $L1_2$ compounds.

According to Wee, Noguchi, Oya & Suzuki[26] for the Ni-based alloys, the gradient of the positive temperature dependence of strength occurs in the order Ni_3Ge>Ni_3Si>Ni_3Ga>Ni_3Al. They showed that the activation constant is a suitable parameter for comparing the propensities of different alloys to show anomalous behavior. Compounds showing an anomalous temperature dependence like Cu_3Au and Ni_3Ge are highly anisotropic. Ni_3Ge has a higher APB energy on the glide planes.

Suzuki, Oya & Ochiai[30] also concluded that in the $L1_2$ compounds having more strongly positive temperature dependence, the extent of homogeneity range tends to be displaced from stoichiometry towards the majority component and the interatomic distance tends to decrease.

The temperature dependence of strength, positive or negative, is not controlled by the APB energy itself but by its anisotropy e.g Ni_3Fe, Ir_3Cr having negative temperature dependence are rather isotropic whereas Cu_3Au and Ni_3Ge, having an anomalous temperature dependence are highly anisotropic[39,40]

2.6.4 EFFECT OF BORON DOPING ON Ni_3Ge

Since brittleness of Ni_3Ge has been attributed to the grain boundary fragility,

researchers have tried to find elements that improve grain boundary cohesion and hence improve ductility. B has been shown to improve the ductility of Ni_3Al tremendously so Taub and Briant and others tried to add B to Ni_3Ge but the results were not very encouraging. Taub and Briant[31] showed that the ability of boron to segregate and also its ability to improve cohesion depend on the total composition of the compound. The presence of borides on the grain boundaries enhanced brittle fracture, but their ability to do so depended on the composition of the alloy.

Taub and Briant[31] worked on five compounds Ni_3Al, Ni_3Ga, Ni_3Si, Ni_3Ge, and Pt_3Ga. B was seen to have a much lower solubility in Ni_3Si and Ni_3Ge than in Ni_3Al. The segregation in these two compounds is also less. They showed that boron was very effective in improving ductility in Ni_3Ga, less so in Ni_3Si and least of all in Ni_3Ge.

The results showed that boron can improve ductility in various Ni_3X compounds but that this effect can be counteracted by the presence of grain boundary precipitates. Also, the total composition of the compound affects the ability of boron to make this improvement.

Since boron is a group III element in the periodic chart, it appears to be most effective in improving cohesion when the non-transition metal in the $L1_2$ compound is also from group III(Al, Ga). Carbon is from group IV and appears to be most effective in improving cohesion when the non-transition metal is from group IV[31].

Eberhart and Vvedensky[32] obtained similar results. They showed that B is effective in improving the ductility in Ni_3Ga and Ni_3Si as well as Ni_3Al but Ni_3Ge remained brittle. They proposed a model for ductility enhancement in $L1_2$ intermetallic

compounds. In their model they have tried to explain the effect of boron doping on the ductility of polycrystalline Ni_3X. Also their model may be used to identify other possible segregants for those cases (e.g Ni_3Ge) where ductility enhancement has proven elusive.

One immediate consequence of their model is that the electronic charge on the grain boundary of a brittle material (either intrinsic or impurity induced) is more polarizable and thus more responsive to a local perturbation such as a stress. As the electronic polarizability has been correlated with yield strength, a brittle grain boundary is expected to have a lower yield strength than the parent crystal. A cohesive enhancer then raises the yield strength near the grain boundary. In fig 2.12 the boron p-orbital electronegativity has been plotted against the Fermi level of Ni_3X. From this figure it can be concluded that boron should be a cohesive enhancer for Ni_3Al, Ni_3Si, and Ni_3Ga. While boron is not expected to be a cohesive enhancer for Ni_3Ge, electronegativity considerations indicate that carbon is a possible alternative, though complications may arise from the uncertainty in the electronic configuration and thus the p-electron count of carbon.

The Fermi energy of Ni_3X is a function of size, electronegativity, and valence. Thus, the susceptibility to boron doping can be summarized in a single electronic parameter- the energy difference between the boron p-orbital energy and the Ni_3X Fermi energy[32].

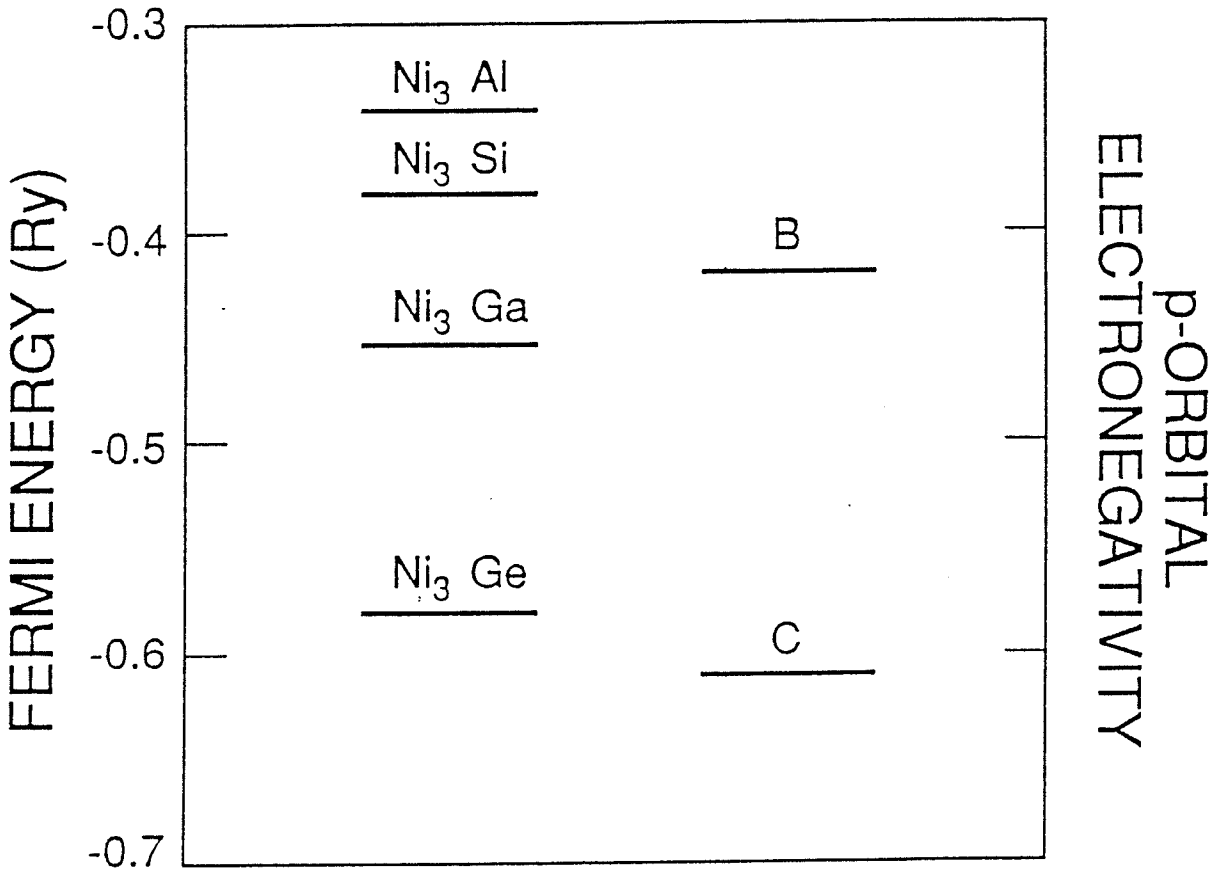

Fig 2.12 The p-orbital electronegativities of B and C compared with the Fermi levels of the brittle polycrystalline materials Ni_3Al, Ni_3Ga, Ni_3Si, and Ni_3Ge[32].

2.6.5 TEMPERATURE DEPENDENCE OF HARDNESS

Westbrook found that the usual temperature dependence of hardness fits two branches of straight lines(fig 2.13). The hardness temperature curve shows a peak. According to Takasugi and Izumi this abnormal behavior is caused by the thermally aided cross slip of screw dislocations on to a cube plane; i.e. the so called Kear-Wilsdorf mechanism. This behavior made these alloys attractive as new heat-resisting materials[33].

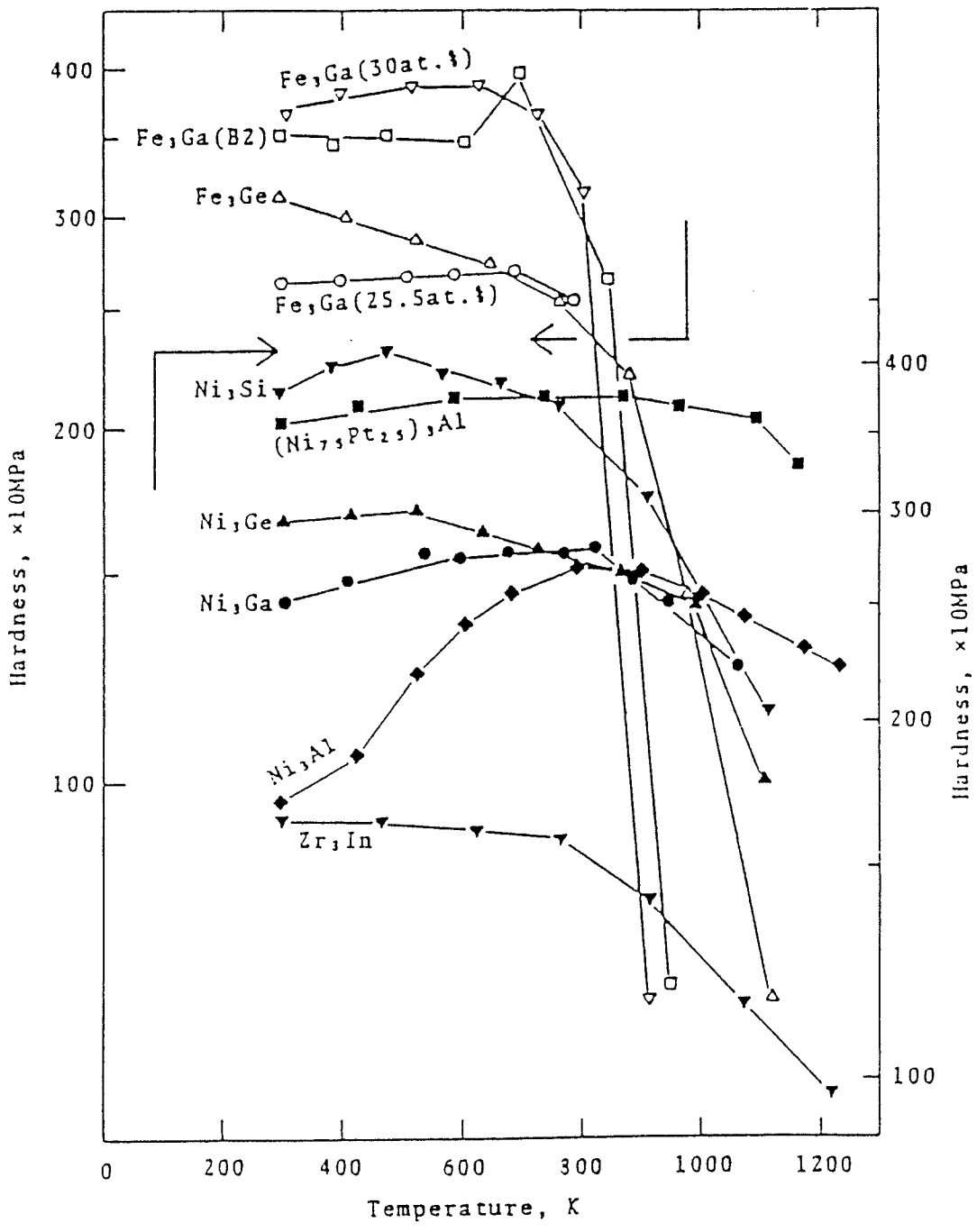

Fig 2.13 Hot hardness curves for $L1_2$ alloys of group 8 transition metals (Fe, Ni) with B-subgroup elements, and for Zr_3Al[33].

2.6.6 Ni_3Ge SINGLE CRYSTALS

Fig 2.14 shows the tensile stress-strain curves of Ni_3Ge single crystals at 290K. From the figure it is observed that Ni_3Ge single crystals exhibit about 5-10% elongation. Failure occurs, however in catastrophic and brittle manner following considerable plastic deformation and necking is not observed (44).

Pak, Saburi, and Nenno made flow stress measurements on single crystals of Ni_3Ge with several different orientations[38]. They observed that the yield stress increases with increasing temperature in the temperature range of -196°C to 800°C where {111} slip operates (positive temperature dependence), but it decreases as {001} slip commences. The critical resolved shear stress for {111}<10-1> slip is orientation dependent. Electron microscope observation on dislocation arrangements in the specimen deformed at -196°C and 27°C has revealed that the mobility of screw dislocations decreases with increasing temperature. These observations indicate that the positive temperature dependence of the yield stress is controlled by the mobility of screw dislocations . This decrease of mobility leading to the positive temperature dependence of the yield stress can be explained by thermally activated cross slip of screw dislocations from the (111) plane to the (010) plane.

Aoki and Izumi (44) observed that failure of intermetallic compound Ni_3Ge single crystals at 290K occurs in a catastrophic and brittle manner after considerable plastic deformation. River lines and cleavage steps which are characteristic of cleavage fracture were seen. Thus, they considered the cleavage fracture of Ni_3Ge to be related to the

decrease of mobile dislocation density by a dislocation pinning mechanism based on the cube cross-slip which causes the positive temperature dependence of the yield stress.

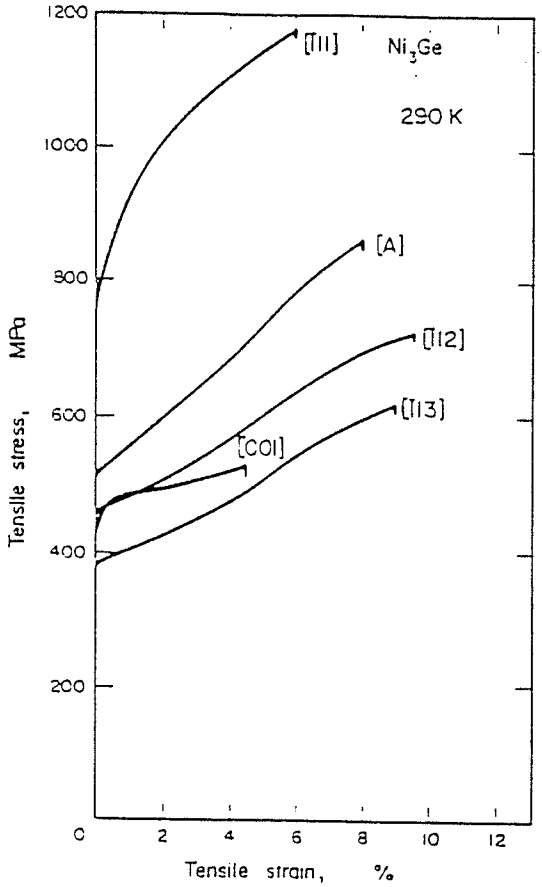

Fig. 2.14 The tensile stress-strain curves of Ni_3Ge single crystals at 290 K.

[A] orientation is located on the [001]-[111] symmetry line and 11deg apart from [111] to [001] orientation.

2.7 Ni-Ge SYSTEM

From the phase diagram (fig 2.15) it can be seen that Ni-Ge is a complex system with a number of invariant reactions, but is still not considered well established, particularly from 20 to 50 at% Ge[34]. All the different reactions occurring in this system are listed in table 2.3.

The maximum solid solubility of germanium in nickel is 16at% at 1124°C. The solubility of nickel in germanium is greatest at 875°C (1.8×10^{-5} at% Ni) and decreases to $4.5X10^{-7}$at%Ni at 700°C[34]. β Ni_3Ge forms congruently at 24 at% Ge, with a homogeneity range of 22.5 to 25 at% Ge over the complete temperature range. ε Ni_5Ge_3 has a maximum homogeneity range of 33.8 to 43.2 at% Ge at 850°C, but this range varies with temperature.

Ruttewit and Masing[35] found that an increase in the Ge content from 1.2 to 6.65at% increases the lattice constant from 0.3526 to 0.3535nm, while a Ge content of 10.87at% raises the lattice constant to 0.3543nm. Nickel solubility in solid germanium is slight.

Alloys of the Ge-Ni system containing a solid solution of germanium in nickel were found to have magnetic properties. Ni_3Ge crystallizes according to Cu_3Au structure type in which Ge atoms are located at the cell corners of the cube octahedra while Ni atoms are positioned at the center of the lattice face.

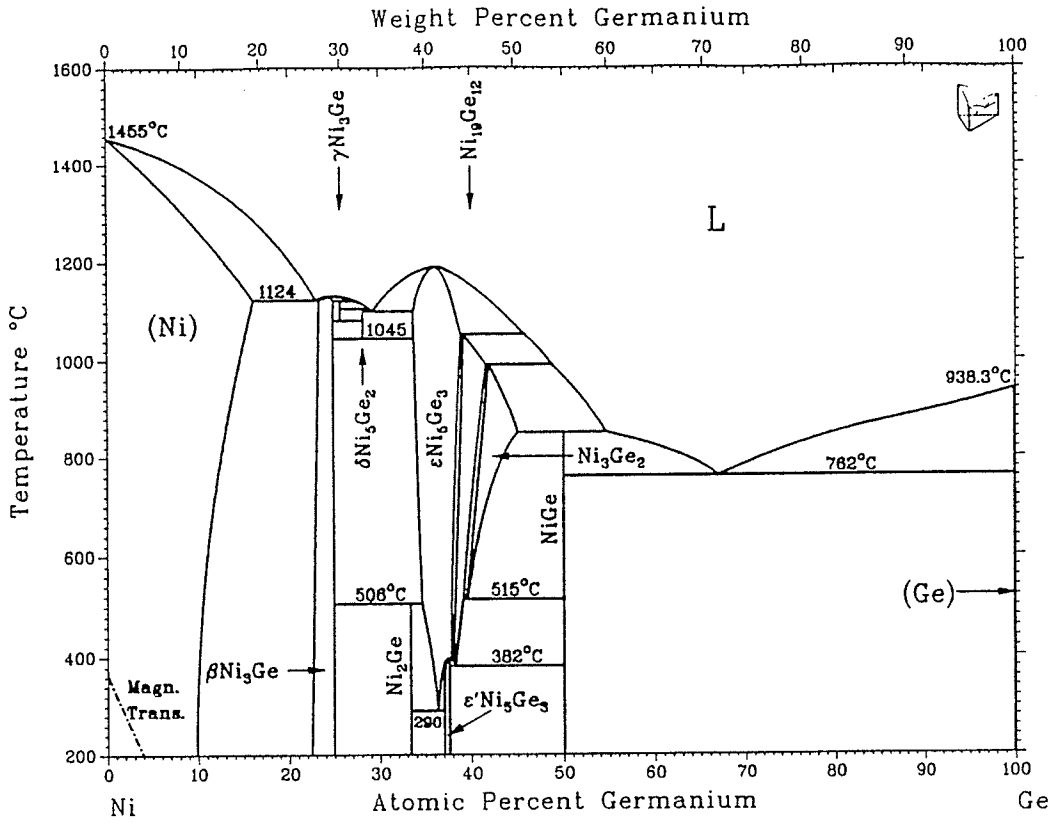

Fig 2.15 Phase diagram of Ni-Ge system

Invariant Reactions in the Ni-Ge System

Reaction	Composition, at.% Ge			Temperature, °C	Reaction type
$L \rightleftarrows (Ni) + \beta Ni_3Ge$	23	~16	~23.3	1124	Eutectic
$L \rightleftarrows \beta\ Ni_3Ge$		~24		1132	Congruent
$L + \beta Ni_3Ge \rightleftarrows \gamma Ni_3Ge$	27.3	~25	~25.6	1118	Peritectic
$L + \gamma Ni_3Ge \rightleftarrows \delta Ni_5Ge_2$	28.9	25.6	28	1102	Peritectic
$\gamma Ni_3Ge \rightleftarrows \beta Ni_3Ge + \delta Ni_5Ge_2$	25.6	~25	28	1082	Eutectoid
$\delta Ni_5Ge_2 \rightleftarrows \beta Ni_3Ge + \epsilon Ni_5Ge_3$	28	25	33.6	1045	Eutectoid
$L \rightleftarrows \delta Ni_5Ge_2 + \epsilon Ni_5Ge_3$	29	28	33.6	1099	Eutectic
$\beta Ni_3Ge + \epsilon Ni_5Ge_3 \rightleftarrows Ni_2Ge$	25	34.5	33.5	506	Peritectoid
$\epsilon Ni_5Ge_3 \rightleftarrows Ni_2Ge + \epsilon' Ni_5Ge_3$	36.3	33.5	37	290	Eutectoid
$L \rightleftarrows \epsilon Ni_5Ge_3$		36.5		1185	Congruent
$L + \epsilon Ni_5Ge_3 \rightleftarrows Ni_{19}Ge_{12}$	~45.5	38.8	39	1050	Peritectic
$L + Ni_{19}Ge_{12} \rightleftarrows Ni_3Ge_2$	47	~41.5	~41.7	990	Peritectic
$Ni_3Ge_2 + L \rightleftarrows NiGe$	~45	54.5	50	850	Peritectic
$Ni_3Ge_2 \rightleftarrows Ni_{19}Ge_{12} + NiGe$	~39.6	~39.2	50	515	Eutectoid
$\epsilon Ni_5Ge_3 \rightleftarrows \epsilon' Ni_5Ge_3 + Ni_{19}Ge_{12}$	~37.7	~37.5	~38	~394	Eutectoid
$Ni_{19}Ge_{12} \rightleftarrows \epsilon' Ni_5Ge_3 + NiGe$	~38.2	~37.6	50	382	Eutectoid
$L \rightleftarrows NiGe + (Ge)$	67	50	~100	762	Eutectic

Table 2.3

2.8 SCOPE OF THE PRESENT STUDY

In recent years, intermetallics have gained a great deal of attention from researchers all over the world. This is because of some of their properties which make them more advantageous than superalloys and high temperature steels. Until now, most of the work has been concentrated on Ni_3Al and Ti_3Al. Although Ti_3Al has already been used for some aircraft parts others have yet to be made suitable for use. A great success has already been acheived in improving the ductility of Ni_3Al by boron addition. In the case of Ni_3Ge, not much work has been done. Researchers have tried to improve it's ductility by employing similar means as for Ni_3Al, but their attempts have proved futile.

Ni_3Ge increases in strength with temperature upto 1000 MPa compared to only 500 MPa obtainable with Ni_3Al. It's ductility can be improved by various techniques described in the literature. Since B addition did not seem to improve its ductility hence in this project another means of improving ductility has been attempted. It is beleived that two phase structures possess higher ductility. The aim of this investigation is to explore this possibility in two phase structures containing Ni_3Ge in the Ni-Ge system.

SCOPE OF FUTURE WORK

(1) Boron additions increase ductility of Ni_3Al by segregation to GB. B in Ni_3Ge does segregate to the grain boundary but has no effect on ductility and precipitates as borides along grain boundary.

One could explore the role of smaller amounts of B on Ni_3Ge such that there

are no precipitates at the GB.

(2) One theory predicts that C addition might improve the ductility of Ni_3Ge but this has to be investigated.

(3) Substitutional solutes such as Ti, Al might reduce electronegativity and improve ductility.

(4) Elements like Ti and Zr may eliminate traces of harmful impurities and increase ductility.

(5) A decrease in grain size generally improves ductility and this has to be tried.

(6) Variation of lattice parameter with temperature and composition give indication regarding the state of order in the material which might control the ductility. This route is yet to be explored.

CHAPTER III

EXPERIMENTAL PROCEDURE

3.1 ALLOY PREPARATION AND HEAT TREATMENT

All the alloys were prepared from a master alloy containing 50wt%Ni and 50wt%Ge. Nickel was 99.99% pure and germanium was 99.999% pure. This alloy was homogenised at 650°C for two weeks and then alloys with composition Ni-20at%Ge, Ni-22.5at%Ge, Ni-23.5at%Ge, Ni-25at%Ge, Ni-27.5at%Ge, and Ni-30at%Ge were prepared by adding more nickel to the master alloy. All alloys were melted in an induction furnace under an argon atmosphere. All these alloys were given a solutionizing heat treatment as listed in table 3.1. To prevent any surface oxidation, all the samples were sealed in quartz tubes under vacuum prior to heat treatment. After heat treating the samples were quenched in water.

3.2 OPTICAL METALLOGRAPHY

The homogenised samples were mounted and polished to 1μ. These were then etched to reveal the grain boundaries and other features. For etching, a solution of 50% HNO_3(conc.) + 25% glacial acetic acid + 25% distilled water was used and in some cases 50% HCl + 25% glycerine + 25% HNO_3(conc.).

The microstructures of the samples were then observed using a Nikon metallograph with magnifications ranging from 50X to 1000X.

TABLE 3.1: SOLUTIONIZING HEAT TREATMENT

COMPOSITION (at%)	HOMOGENISING TREATMENT
20.0	800°C-39.00hrs 900°C-57.00hrs 1000°C-73.50hrs
22.5	800°C-27.25hrs 900°C-25.75hrs 1000°C-92.00hrs
23.5	800°C-39.00hrs 900°C-57.00hrs 1000°C-73.50hrs
25.0	800°C-28.00hrs 900°C-42.50hrs 1000°C-72.00hrs
27.5	800°C-24.00hrs 900°C-24.00hrs 1000°C-72.00hrs
30.0	800°C-24.00hrs 900°C-27.00hrs 1000°C-72.00hr

Optical microscopy was also done for deformed samples from the compression test to show the crack initiation and propagation behavior for different compositions under various temperature conditions.

3.3 SCANNING ELECTRON MICROSCOPY

SEM was used to analyse the different phases present in the samples and to do fractography of the failed samples. For chemical analysis, EDS was used. A minimum of ten measurements was made for each phase. The MicroQ program of the Tracor Northern EDS system was used to do point analysis which gives better accuracy.

Fractography was done to identify the mode of fracture. To draw any useful conclusions from the photographs it is essential that they are taken at different magnifications for the same area and at the same tilt angle. This was taken into consideration in taking the photographs.

3.4 MICROHARDNESS

To measure the hardness of the individual phases microhardness measurements were made on a Vickers hardness testing machine. Loads were selected on the basis of the hardness of the phases. A minimum of 8-10 measurements was made for each phase.

3.5 QUANTITATIVE METALLOGRAPHY

For each specimen, the volume fraction of precipitate and the grain size were measured. This was done on a Leitz TAS plus image analyser.

GRAIN SIZE MEASUREMENT: The grain boundaries in most of the samples were not clearly visible and the contrast between the phases was not very good. Therefore, for accurate results the grain boundaries were traced from photographs taken in 6-10 different areas. The final grain size was obtained by taking an average.

VOLUME PERCENT MEASUREMENT:

(a) AUTOMATIC PROGRAM: For two phase material, first both the phases have to be identified in order for the program to work. It takes a number of fields and the final value is an average of all these.

(b) MANUAL PROGRAM: In this a central point is located on the screen and the counting is done based on your identification of the phase in which this point lies. After certain number of points the volume percent value stops changing and this becomes the final answer.

3.6 MACROHARDNESS

To get an idea of the overall hardness of the material, macrohardness measurements were done. Hardness at ten different points was measured to avoid any error. This was done on Vickers hardness machine. Loads were selected on the basis of the material.

3.7 X-RAY DIFFRACTION

To identify the various phases present and to get a precise value for the lattice parameter, X-Ray diffraction was done for all the samples. For this, powder was made from the bulk material by filing. This filed powder was ground again to get 325mesh size particles. Since some strains are introduced into the material while filing and grinding, the material was annealed at 1000°C for 5 mins to remove these stresses and thus avoid peak broadening in the diffraction pattern. Before heat treating the powder was sealed under vacuum to avoid oxidation.

The powder was then mixed with silicon standard and spread uniformly on a glass plate with help of acetone. The samples were run from 10° to 140° 2θ at a speed of 6 deg/min.

The data were recorded automatically on an attached terminal. After identifying the Si peaks and the alloy peaks the lattice parameter was calculated by using the Celref program. The program makes 2θ corrections by using the standard peaks and modifies the approximate initial values of the lattice parameter.

3.8 COMPRESSION TEST

Sample description

Since the material is very brittle and hence difficult to machine, the samples were cast in the form of 6mm cylinders. These were then given the same annealing treatment. To avoid buckling or barreling, the ideal length to diameter ratio should be 1.56 according to ASM metals handbook. Therefore, according to the diameter, the samples were cut to

a length of 1-1.2cm to maintain this ratio. These were then polished to 600 grid emery paper to render the surfaces smooth.

Test conditions

These specimens were then tested under compression on the universal testing machine. Each alloy was tested at a variety of temperatures ranging from RT to 600°C and each test was repeated 2 to 3 times to determine the accuracy. At higher temperatures, graphite lubrication was applied on both faces of the sample to prevent barreling and the experiments were performed under argon atmosphere. Before starting the tests the samples were soaked at the test temperature for at least one hour.

All the tests were done at a constant strain rate of 2.0×10^{-4} s^{-1}. To determine strain, the cross head position was measured with an LVDT. The samples were furnace cooled to RT after the test.

3.9 TRANSMISSION ELECTRON MICROSCOPY

Thin discs (≈ 1mm) were cut from the material and then polished on emery paper to a thickness of 0.1μm. Then, on a spark machine discs with a diameter of 3mm were cut. The discs were then polished using a grinder to 40-50μ. After this, dimples were made at the centres of these discs to further reduce the thickness to 20-30μ. This dimpling helps in reducing the time required to obtain a hole on the ion-beam milling machine.These dimpled samples were put in the ion-beam milling machine for 2-3hrs until a hole was obtained. While polishing, the beam direction was gradually changed

from 15° to 10°. to get a larger thin area around the hole.

The thinned samples were then observed in a JEM-2000 FX electron microscope which uses a tungsten filament for electron generation with a probe size of 50nm. An accelerating voltage of 200kV was used for all samples.

CHAPTER IV

RESULTS

4.1 PART I : CHARACTERIZATION OF THE SAMPLES

Samples with composition Ni-20.0 at%Ge, Ni-22.5 at%Ge, Ni-23.5 at%Ge, Ni-25.0 at%Ge, Ni-27.5 at%Ge, and Ni-30 at%Ge were characterized prior to mechanical testing. This helps in understanding the mechanical behavior exhibited by the samples.

Optical metallography results are shown in figs.4.1 to 4.6. Fig 4.1 shows that Ni-20 at%Ge still retains the dendritic structure after heat treatment. Extending heat treatment to two weeks at 1000°C did not change the structure. Heat treating the samples after deforming them at 200°C did not remove the dendritic structure. This implies that for this composition it is very hard to break the dendritic structure. According to the phase diagram this composition consists of (Ni)+Ni_3Ge and since one is ordered and the other disordered hence the reason might be the low diffusion rates in ordered phase.

For the composition Ni-22.5 at%Ge it is seen from fig 4.2 that there is a distribution of concentrated regions of lamellar structure. These consist of (Ni) and Ni_3Ge lamellae forming in Ni-rich regions. The matrix consists of Ni_3Ge phase.

According to the phase diagram, Ni-23.5 at%Ge and Ni-25.0 at%Ge should consist of single phase Ni_3Ge but from Fig 4.3 and 4.4 it is seen that there is a second phase at the grain boundary. From EDS analysis it was found that this is a phase high in germanium and hence its occurrence can be attributed to slight deviation from the nominal composition. It is also observed from the two figures that the grains for the

composition Ni-25.0 at% Ge are elongated whereas for Ni-23.5 at% Ge they are almost equiaxed. The differences might be because of a difference in composition or different cooling rates.

Microstructures of alloys of compositions Ni-27.5 at% Ge and Ni-30 at% Ge show the presence of two phases(figs 4.5 and 4.6) which should be Ni_5Ge_3 and Ni_3Ge as is evident from the phase diagram and confirmed by EDS analysis. But since they were water quenched after heat treatment one of the phases shows a needle-like structure characteristic of martensite. Ni_5Ge_3 precipitation occurs at the grain boundaries of Ni_3Ge.

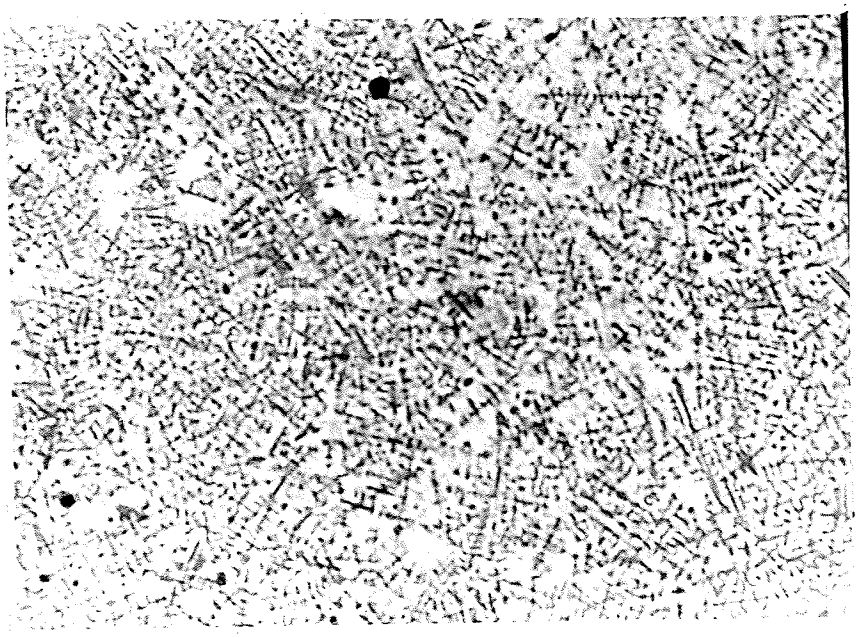

Fig 4.1 Ni-20 at% Ge Homogenised (50X)

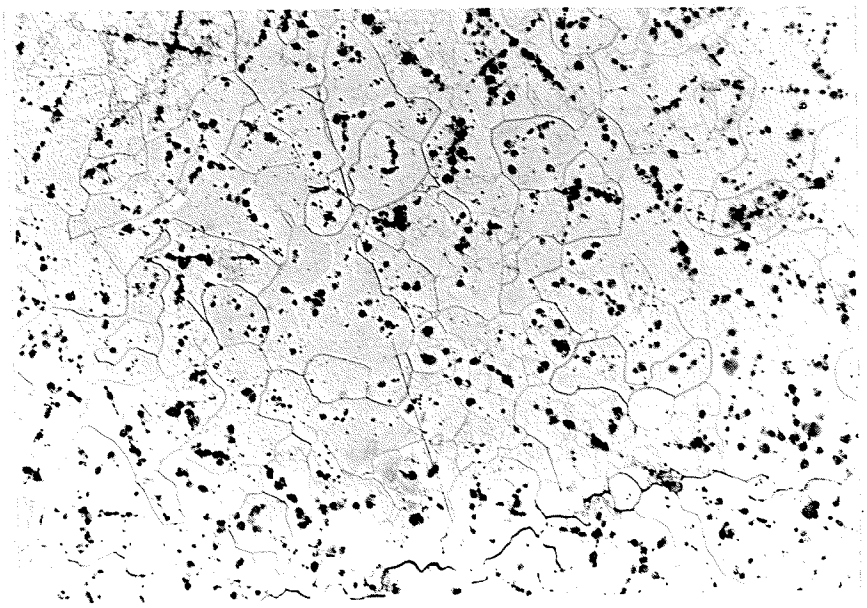

Fig 4.2 Ni-22.5 at% Ge Homogenised (50X)

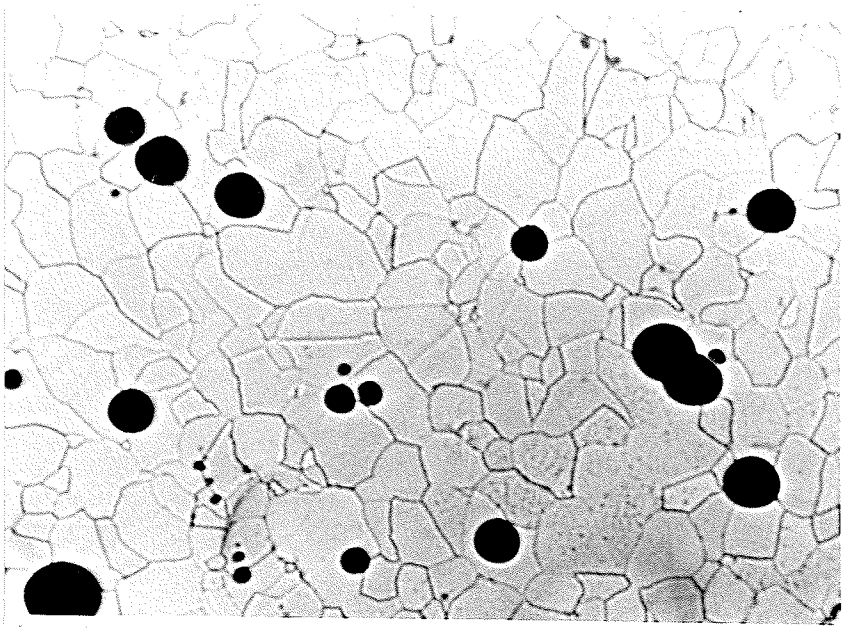

Fig 4.3 Ni-23.5 at% Ge Homogenised (50X)

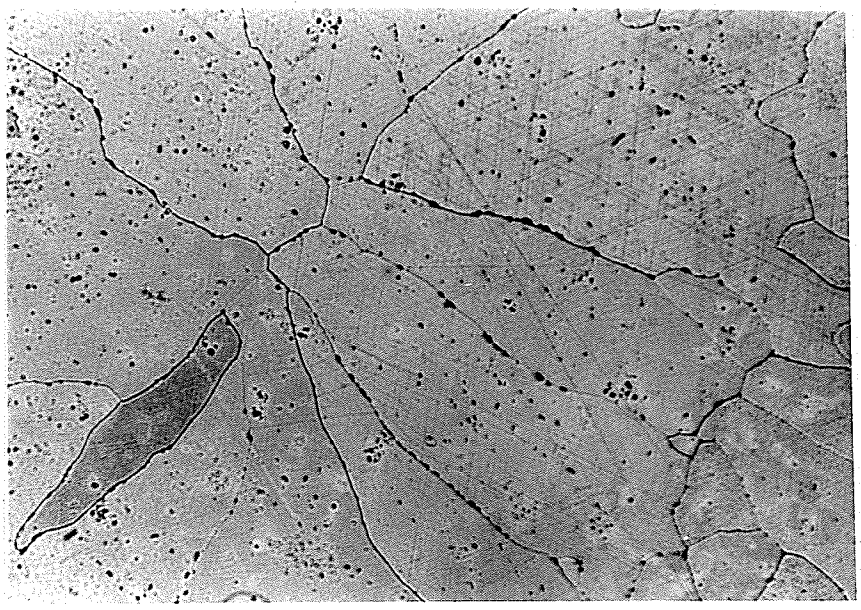

Fig 4.4 Ni-25.0 at% Ge Homogenised (50X)

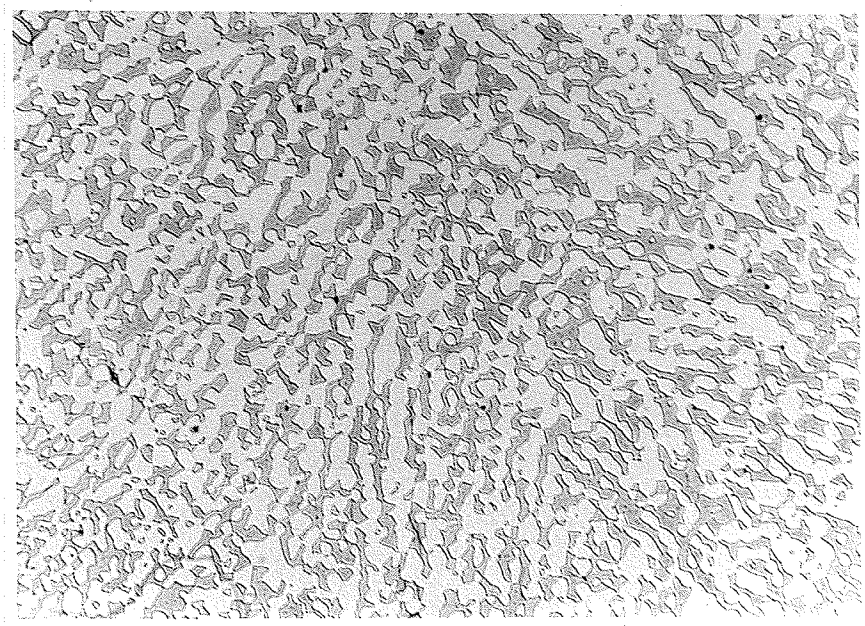

Fig 4.5 Ni-27.5 at% Ge Homogenised (50X)

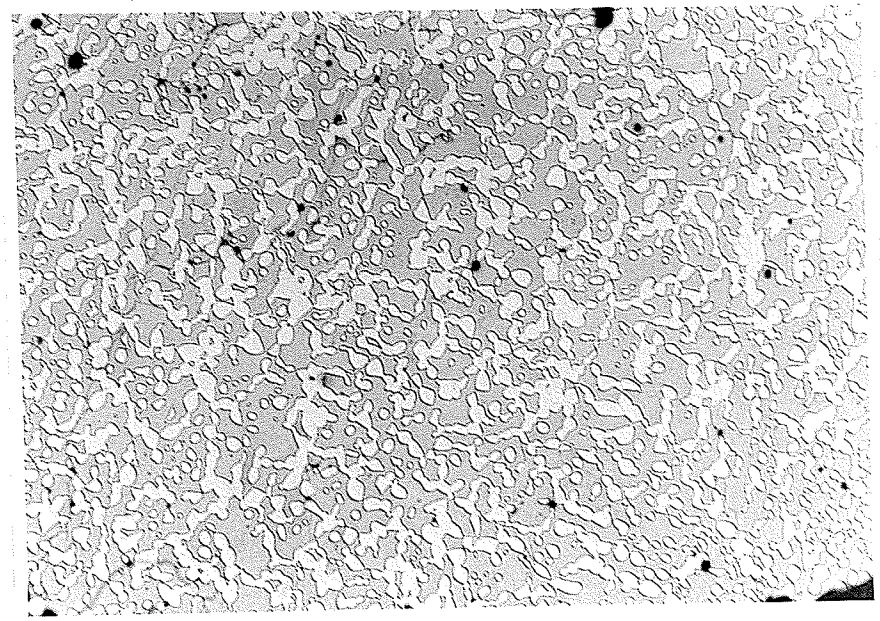

Fig 4.6 Ni-30.0 at% Ge Homogenised (50X)

Table 4.1 gives the EDS analysis data of all the samples. Also listed are the expected phases from the phase diagram and their compositions. On comparing the two we find that they all match within 5% experimental error.

Table 4.2 gives the microhardness and macrohardness measurements of all the alloys. For Ni-20.0 at% Ge and Ni-22.5 at% Ge one of the phases was very dark and hence microhardness measurements were not possible. From the results it is seen that the microhardness of the phases increases in the order (Ni), Ni_3Ge, and lastly Ni_5Ge_3. Macrohardness results shows that if we compare the hardnesses of all the alloys with Ni_3Ge then it becomes evident that on adding more Ni to Ni_3Ge the hardness value goes down. Whereas introducing Ni_5Ge_3, by adding more germanium, makes the material harder. These observations are quite consistent with the microhardness results. Thus, we can say that the hardness of an alloy can be modified by introducing a second phase and is dependent upon the morphology, distribution, and volume percent of the second phase.

Volume fraction measurements(table 4.3) on the image analyser deviated considerably from the expected values, the reason might be the low contrast between the two phases.

Porosity in the samples, perhaps resulting from inadequacies in the melting and casting technique, might be a factor affecting the properties to a great extent. Porosity was measured by comparing the theoretical density with the experimental measurements. It was found that maximum porosity was present in pure Ni_3Ge which was about 5%. But for Ni-27.5 at% Ge and Ni-30 at% Ge the porosity was about 0.2%.

Grain size measurements (table 4.4) showed that Ni-27.5at%Ge and Ni-30.0at%Ge have considerably smaller grain size compared to other compositions. Also, the two phases are uniformly distributed.

Lattice parameter results are listed in table 4.5. Most of the (Ni) and Ni_3Ge peaks overlapped and therefore only a few of the peaks which did not overlap were utilized and the lattice parameter of Ni_3Ge was calculated based on these peaks. Since Ni-23.5 at% Ge and Ni-25.0 at% Ge are single phase all the peaks were taken into account in calculating the lattice parameter. For Ni-27.5 at% Ge and Ni-30.0 at% Ge most of the peaks corresponded to Ni_3Ge and with extra peaks having a very low intensity. These extraneous peaks perhaps due to impurities were ignored in the calculation of lattice parameter for Ni_3Ge.

TABLE 4.1 EDS ANALYSIS ON SEM

COMPOSITION	CHEMICAL ANALYSIS	PHASES & COMPOSITION FROM PHASE DIAGRAM	%MATCHING
Ni-20at%Ge	white:Ni14.47Ge	(Ni):Ni-14.5Ge	0.2%
	dark:Ni-22.25Ge	Ni_3Ge:Ni-23.2Ge	4.0%
Ni-22.5at%Ge	white:Ni15.18Ge	(Ni):Ni-14.5Ge	4.7%
	dark:Ni-22.29Ge	Ni_3Ge:Ni-23.2Ge	3.9%
Ni-23.5at%Ge	white:Ni-23.1Ge	Ni_3Ge:Ni-23.5Ge	1.7%
	GBppt:Ni24.2Ge		
Ni-25.0at%Ge	white:Ni24.55Ge	Ni_3Ge:Ni-25.0Ge	1.8%
	GBppt:Ni29.0Ge		
Ni-27.5at%Ge	white:Ni-24.8Ge	Ni_3Ge:Ni-25Ge	0.8%
	dark:Ni-34.14Ge	Ni_5Ge_3:Ni33.7Ge	1.3%
Ni-30.0at%Ge	white:Ni24.88Ge	Ni_3Ge:Ni-25Ge	0.48%
	dark:Ni-34.18Ge	Ni_5Ge_3:Ni33.7Ge	1.42%

TABLE 4.2 MICROHARDNESS & MACROHARDNESS

COMPOSITION	MICROHARDNESS (DPH)	MACROHARDNESS (VHN)
Ni-20.0at%Ge	(Ni):not possible Ni_3Ge:381	299
Ni-22.5at%Ge	(Ni):not possible Ni_3Ge:406	296
Ni-23.5at%Ge	Ni_3Ge:423	313
Ni-25.0at%Ge	Ni_3Ge:508	371
Ni-27.5at%Ge	Ni_3Ge:501 Ni_5Ge_3:841	473
Ni-30.0at%Ge	Ni_3Ge:486.87 Ni_5Ge_3:857.25	549

TABLE 4.3: VOLUME FRACTION MEASUREMENTS

COMPOSITION	VOLUME FRACTION FROM PHASE DIAGRAM	VOLUME FRACTION (EXPERIMENTAL)	%DEVIATION
Ni-20at%Ge	Ni_3Ge:0.63 (Ni):0.37	Ni_3Ge:0.67 (Ni):0.33	6.35 10.80
Ni-22.5at%Ge	Ni_3Ge:0.92 (Ni):0.08	Ni_3Ge:0.94 (Ni):0.06	2.20 25.00
Ni-23.5at%Ge	Ni_3Ge:1.00	Ni_3Ge:1.00	0.00
Ni-25.0at%Ge	Ni_3Ge:1.00	Ni_3Ge:1.00	0.00
Ni-27.5at%Ge	Ni_3Ge:0.71 Ni_5Ge_3:0.29	Ni_3Ge:0.63 Ni_5Ge_3:0.37	11.27 27.57
Ni-30.0at%Ge	Ni_3Ge:0.42 Ni_5Ge_3:0.58	Ni_3Ge:0.46 Ni_5Ge_3:0.54	9.5 6.9

TABLE 4.4: GRAIN-SIZE MEASUREMENT

COMPOSITION	GRAIN-SIZE(m)
Ni-20.0at%Ge	Not possible
Ni-22.5at%Ge	155
Ni-23.5at%Ge	113.7
Ni-25.0at%Ge	313.92
Ni-27.5at%Ge	31.57
Ni-30.0at%Ge	25.66

TABLE 4.5: X-RAY LATTICE PARAMETER VALUES OF Ni_3Ge

COMPOSITION	LATTICE PARAMETER (EXPERIMENTAL)§	LATTICE-PARAMETER (THEORETICAL)§	%DEVIATION
Ni-20.0at%Ge	3.57218	3.5731	0.026
Ni-22.5at%Ge	3.57203	3.5731	0.0299
Ni-23.5at%Ge	3.57046	3.5731	0.0739
Ni-25.0at%Ge	3.57377	3.5731	-0.0187
Ni-27.5at%Ge	3.57268	3.5731	0.0117
Ni-30.0at%Ge	3.56965	3.5731	0.0965

4.2 PART II: MECHANICAL TESTING AND INVESTIGATION INTO THE POSSIBLE REASONS FOR THE OBSERVED BEHAVIOR

The presence of the intermetallic compound Ni_3Ge makes all the alloys containing this phase brittle. Hence,the material becomes hard to machine and has almost zero deformability in tension. Thus, to obtain an estimate of strength, compression tests were utilized. Results showed anomalous behavior for all the compositions. An attempt to understand this behavior was made by doing fractography on the failed samples, optical metallography of the deformed samples, and TEM on thin films.

Also, to understand the effect of strain hardening, the macrohardness of the deformed samples was measured. The strain hardening values were calculated using the slopes from the stress-strain curves and the values were plotted against the strain values.

4.2.1 COMPRESSION TESTS

Out of the six compositions, only four were selected for mechanical testing. The selected samples were Ni-22.5 at% Ge consisting of (Ni)+Ni_3Ge, Ni-23.5 at% Ge consisting of single phase Ni_3Ge, Ni-27.5 at% Ge & Ni-30.0 at% Ge both consisting of two phases Ni_5Ge_3 and Ni_3Ge.

To gain an estimate of the scatter in the values for yield stress 2-3 tests were conducted on each specimen at temperatures 21°C, 200°C, 400°C, & 600°C. Also single tests were conducted at intermediate temperatures to further characterize this mechanical behavior. The results showed that the scatter was within 10% of the mean values.

(a) TRUE STRESS vs TRUE STRAIN

The true stress-true plastic strain curves are shown in figs 4.7 and 4.8. At lower temperatures Ni-22.5at%Ge shows considerable deformation (fig 4.7a & 4.7b) but as the temperature goes up it reduces. Ni-30.0at%Ge seems to be quite ductile at all temperatures but the deformation goes up by 40% at high temperatures. Pure Ni_3Ge does not exhibit much ductility.

In case of Ni-22.5 at% Ge strain value shows a drastic decrease at 600°C(fig 4.8a). Ni-23.5 at% Ge shows almost same behavior at both RT and 200°C(fig 4.8b). In case of Ni-27.5 at% Ge deformation is almost same at all temperatures except 600°C where it goes up but the strength value is considerably reduced(fig 4.8c). Maximum stress levels are observed at 200°C.For Ni-30.0 at% Ge the curves flatten out at 400°C and the strain values show a drastic increase but the stress value comes down(fig 4.8d). Thus although both Ni-27.5 at% Ge and Ni-30.0 at% Ge consist of the same phases but their mechanical behavior shows that the volume fraction of the phases play an important role in determining the mechanical properties of the alloy.

(b) STRAIN-HARDENING vs STRAIN

Strain hardening values give a considerable idea about the tendency of the material to work harden under a given load. In this experiment they were calculated using slopes from the true stress-true strain curves at different strain levels. These were plotted against strain to estimate the strain hardening value at each strain level.

At 21°C, Ni-22.5 at% Ge and Ni-30.0 at% Ge show almost the same strain

hardening behavior(fig 4.9a).The maximum strain hardening is observed for Ni-23.5 at% Ge but its rate of decrease with strain is considerably high. Ni-27.5 at% Ge shows an unusual behavior which might be a result of some error in data collection. At 200°C again we see the same behavior for all alloys(fig 4.9b). At higher temperatures we see that Ni-27.5 at% Ge and Ni-30.0 at% Ge both show almost constant strain hardening whereas Ni-22.5 at% Ge shows a very steep drop(fig 4.9d).

Ni-22.5 at% Ge shows almost same behavior upto 400°C and the strain hardening rate shows an initial fall after which it becomes constant. The behavior changes at 600°C and it sharply drops(fig 4.10a). Ni-23.5 at% Ge shows the same behavior at both 21°C and 200°C(fig 4.10b). For Ni-27.5 at% Ge if we ignore behavior at RT then it shows a smooth change from steep fall at 200°C to almost constant behavior at 600°C(fig 4.10c). Ni-30.0at%Ge shows a clear difference between low temperature behavior where it first falls and then smoothens out and then falls again and high tempearture where it is almost flat and does not change much with strain levels(fig 4.10d).

(c) 0.2% YIELD-STRESS vs COMPOSITION:

The graph has been divided into three regions depending on the phases(fig 4.11). We can see that on changing from two phase (Ni)+Ni_3Ge to single phase Ni_3Ge, the strength decreases at all temperatures except at 21°C. This shows that the second phase α strengthens the intermetallic phase at higher temperatures.

On going from single phase Ni_3Ge to two phase Ni_5Ge_3+ Ni_3Ge, it is observed that at lower temperatures the strength goes up but at higher temperatures it goes down. This implies that Ni_3Ge becomes stronger at higher temperatures. Ni_5Ge_3 strengthens the Ni_3Ge

phase at lower temperatures. Increasing the volume fraction of Ni_5Ge_3 does not make much difference in the strength level.

(d) 0.2% YIELD-STRESS vs TEMPERATURE

All four alloys were seen to exhibit anomalous behavior. The difference was the maximum yield strength and the temperature at which it occurs. Fig 4.12 shows the variation of yield strength with temperature for all the four alloys. It is seen that the presence of Solid solution of Ge in Ni(α) along with Ni_3Ge increases the yield strength tremendously and also increases the peak strength temperature. Ni_5Ge_3 phase slightly increases the peak strength temperature but brings down the peak yield strength temperature.

(e) % TRUE PLASTIC STRAIN vs COMPOSITION:

Here also the region has been divided into three depending on the phases(fig 4.13).It shows that as the composition goes from (Ni)+Ni_3Ge to Ni_3Ge the % deformation goes down at all temperatures except 600°C. This shows that Ni_3Ge acheives some degree of plasticity at this temperature and that dislocations can surpass any barriers to their motion easily.

On going from single phase Ni_3Ge to two phase Ni_3Ge+ Ni_5Ge_3 the % deformation goes up. The maximum increase is found at 600°C. Thus the results imply that at 600°C most compositions achieve a considerable degree of plasticity. For α+Ni_3Ge the strain hardening level is quite high thus the deformation is small.

(f) % TRUE PLASTIC STRAIN vs TEMPERATURE:

The curves show an increase in maximum deformation with temperature(fig 4.14) but the degree to which this increase occurs depends on the composition. Upto 200°C there is not much increase but at higher temperatures, the maximum strain increases for all compositions except Ni-22.5 at% Ge. Ni-30 at% Ge shows the maximum increase in deformation. It exhibits 10% deformation at room temperature which increases to 40% at 600°C. Ni-23.5at%Ge also shows a considerable increase in deformation at 600°C.

(g) TOUGHNESS vs COMPOSITION:

Toughness was calculated by measuring the area under the true-stress true-strain curve. The variation with composition(fig 4.15) reveals that minimum toughness is shown by Ni_3Ge at all temperatures and the maximum by two phase Ni_3Ge+ Ni_5Ge_3 at all temperatures.

(h) TOUGHNESS vs TEMPERATURE:

Variation in toughness with temperature is shown in fig 4.16. It shows that for Ni-27.5 at% Ge the value remains almost constant at all temperatures. For Ni-22.5 at% Ge it shows a peak at 200°C and for Ni-30.0 at% Ge it shows a substantial increase at 600°C. The data for Ni-23.5 at% Ge were insufficient to predict any variation.

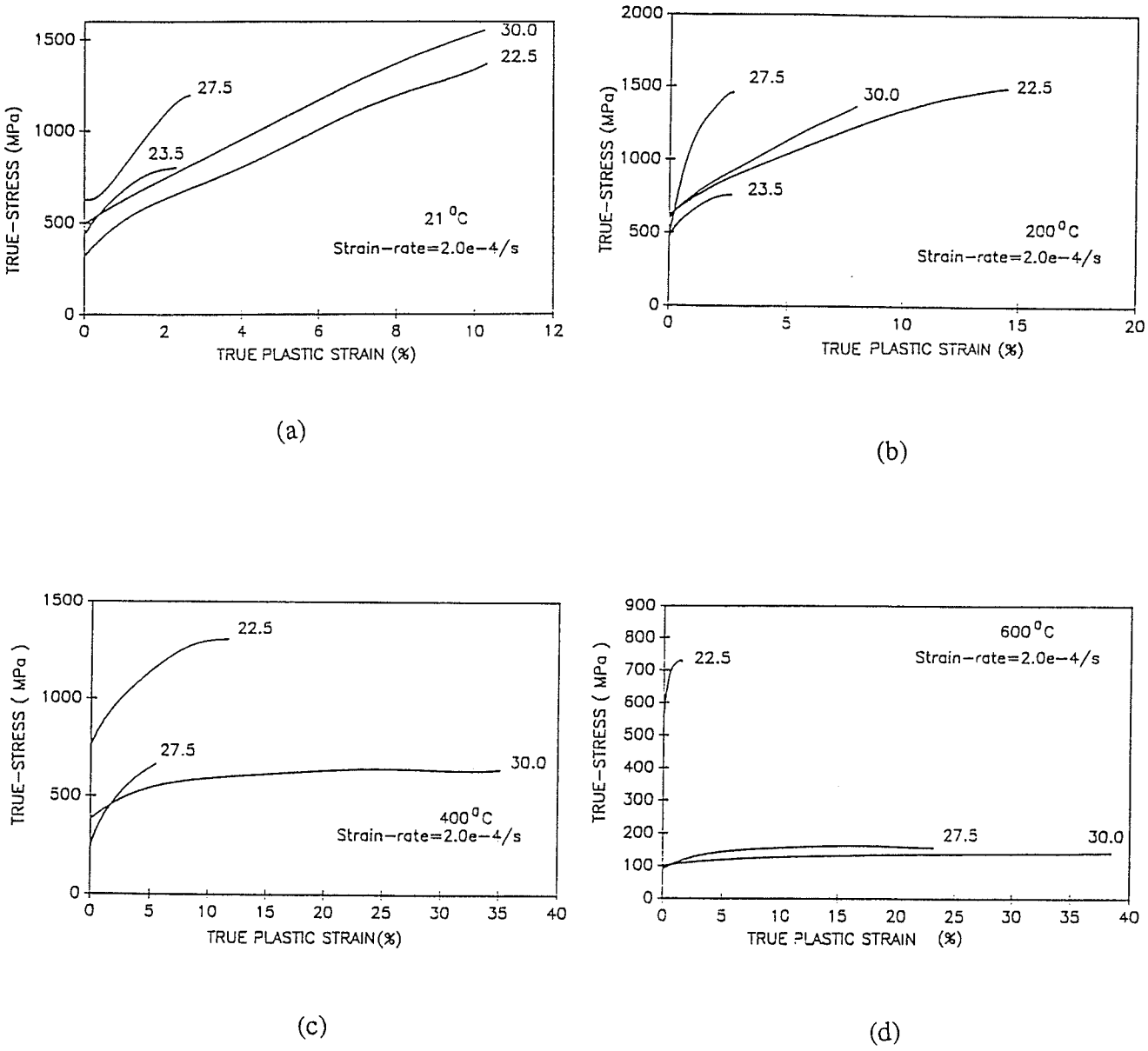

Fig 4.7 True-stress vs true plastic strain for compositions Ni-22.5at%Ge, Ni-23.5at%Ge, Ni-27.5at%Ge, and Ni-30.0at%Ge at (a)21°C (b)200°C (c)400°C (d)600°C

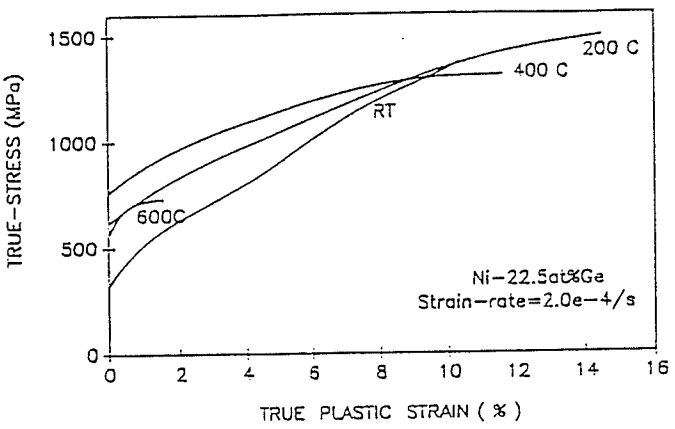

(a)

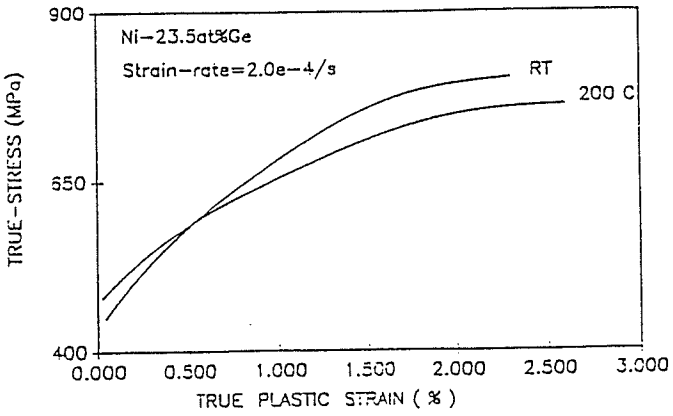

(b)

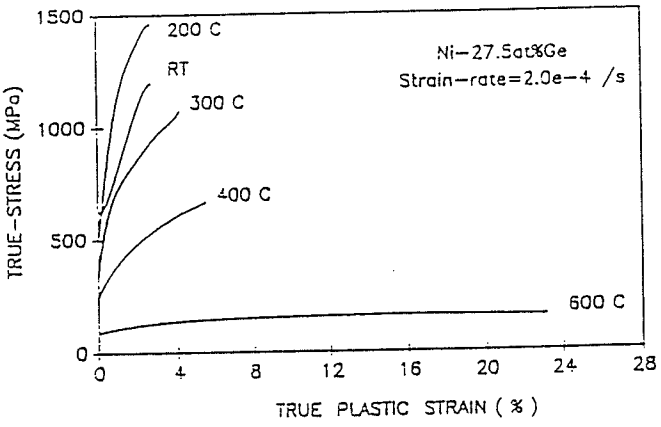

(c)

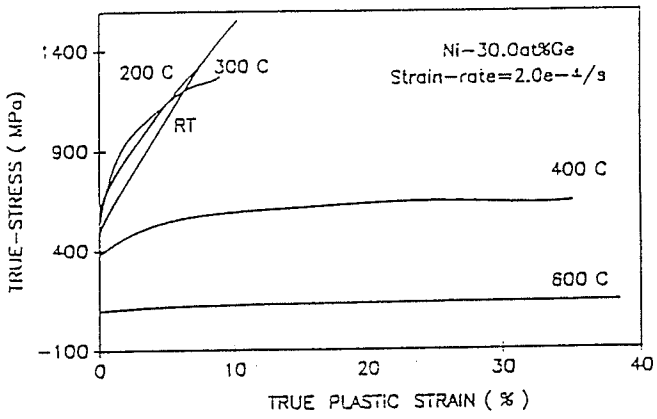

(d)

Fig 4.8 True-stress vs true plastic strain at temperatures 21°C, 200°C, 400°C, and 600°C for (a) Ni-22.5at%Ge (b) Ni-23.5at%Ge (c) Ni-27.5at%Ge (d) Ni-30.0at%Ge

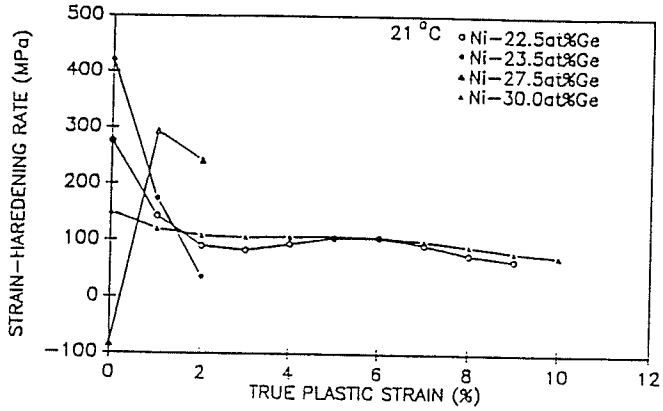

(a)

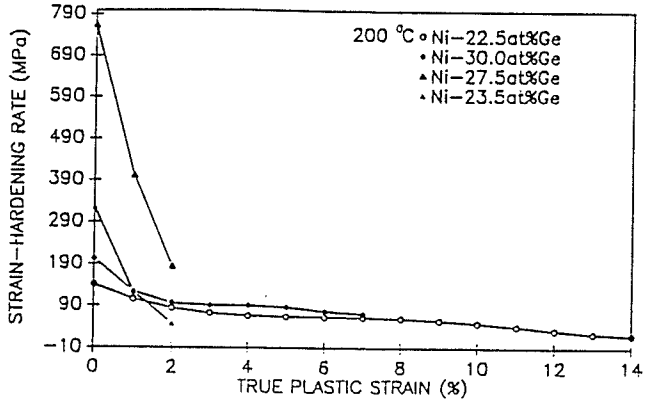

(b)

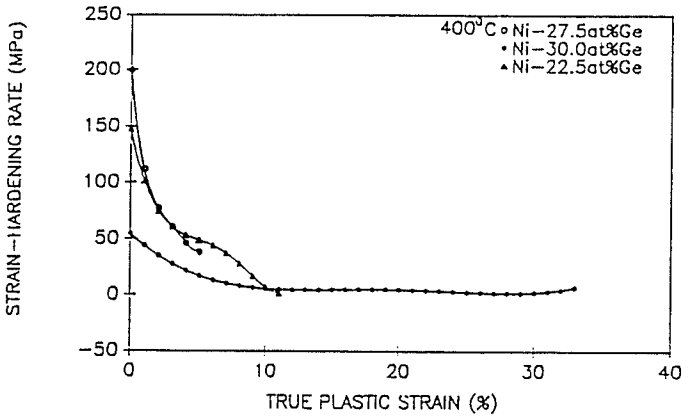

(c)

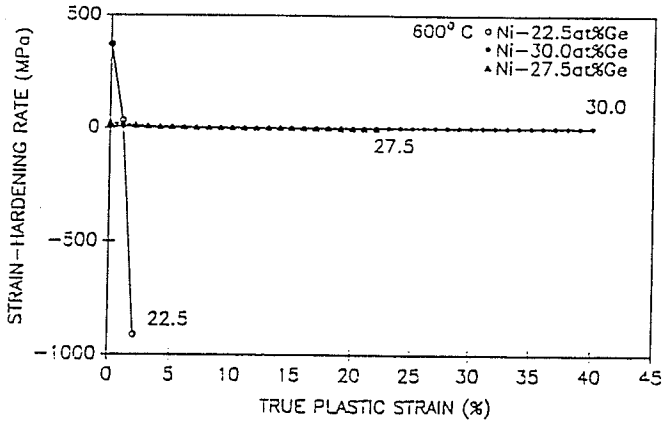

(d)

Fig 4.9 Strain-hardening rate vs true plastic strain for compositions Ni-22.5at%Ge, Ni-23.5at%Ge, Ni-27.5at%Ge, and Ni-30.0at%Ge at (a)21°C (b) 200°C (c) 400°C (d) 600°C.

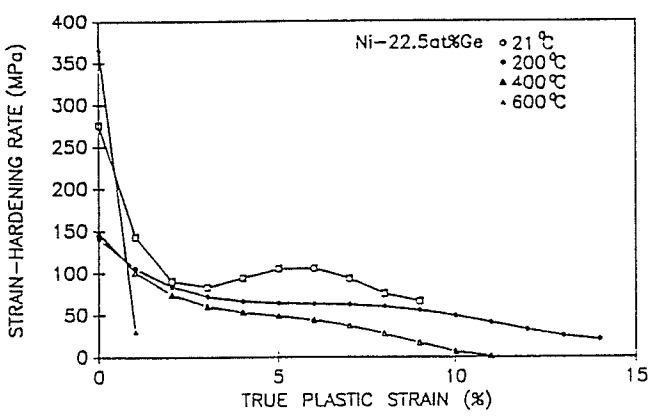

(a)

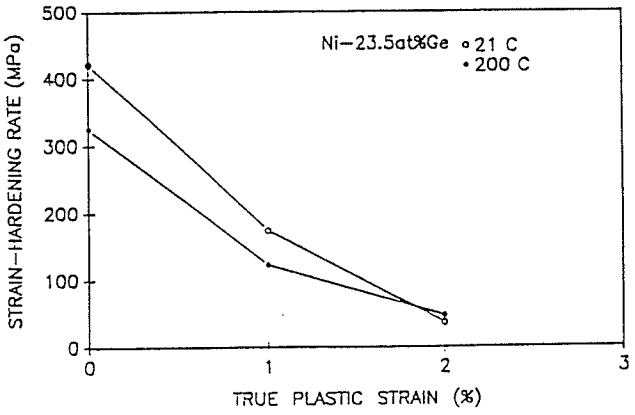

(b)

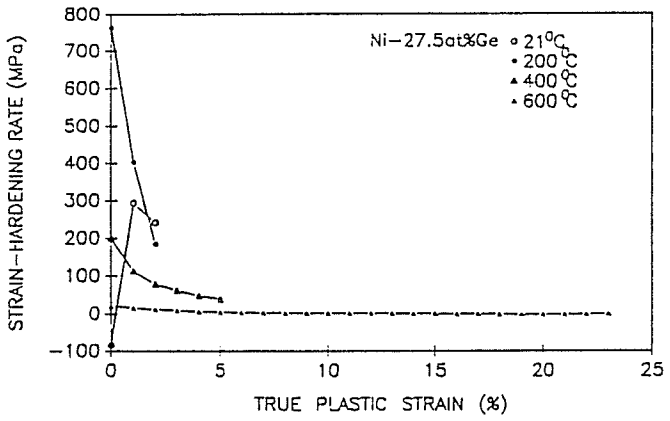

(c)

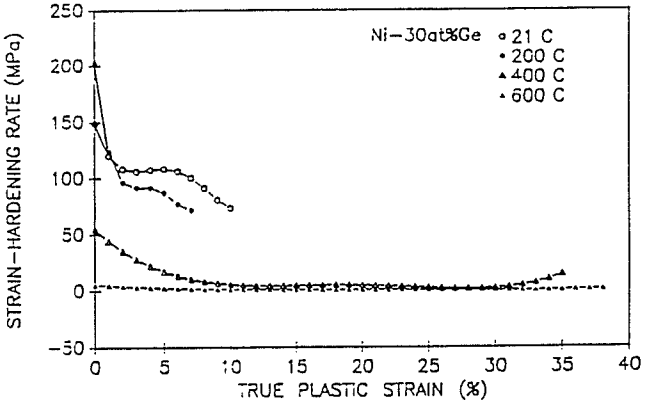

(d)

Fig 4.10 Strain-hardening rate vs true plastic strain at 21°C, 200°C, 400°C, and 600°C for (a) Ni-22.5at%Ge (b) Ni-23.5at%Ge (c) Ni-27.5at%Ge (d) Ni-30.0at%Ge.

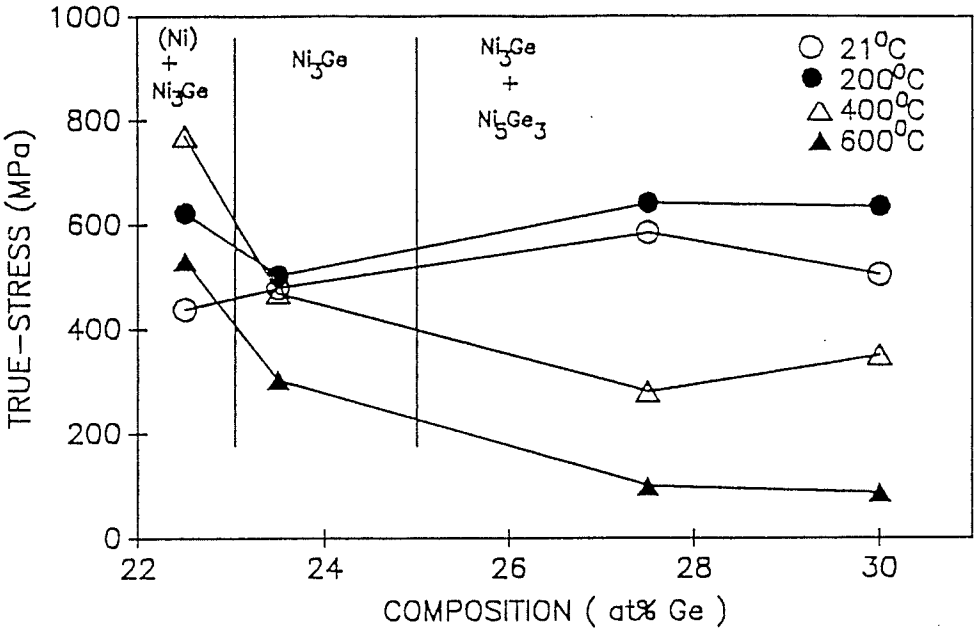

Fig 4.11 0.2%Yield-stress vs composition at 21°C, 200°C, 400°C and 600°C

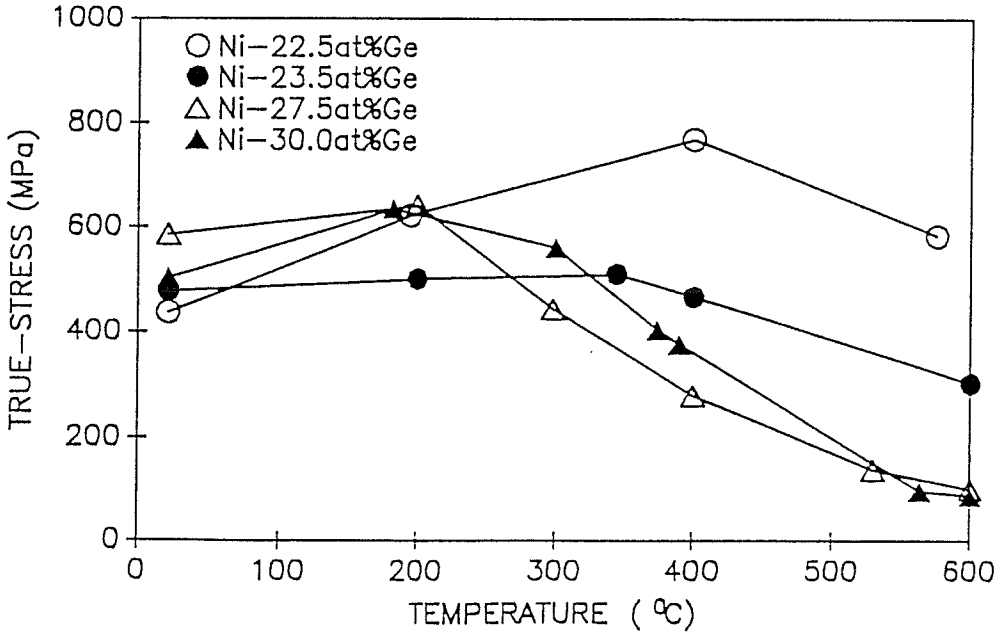

Fig 4.12 0.2%Yield-stress vs temperature for Ni-22.5at%Ge, Ni-23.5at%Ge, Ni-27.5at%Ge, and Ni-30.0at%Ge.

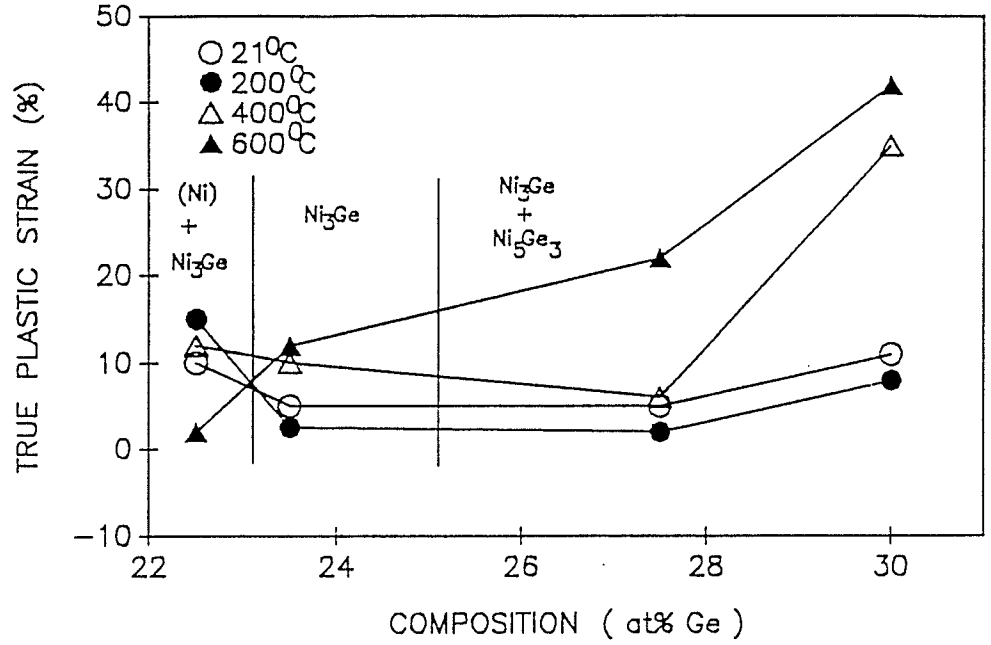

Fig 4.13 True plastic strain vs composition at 21°C, 200°C, 400°C, and 600°C.

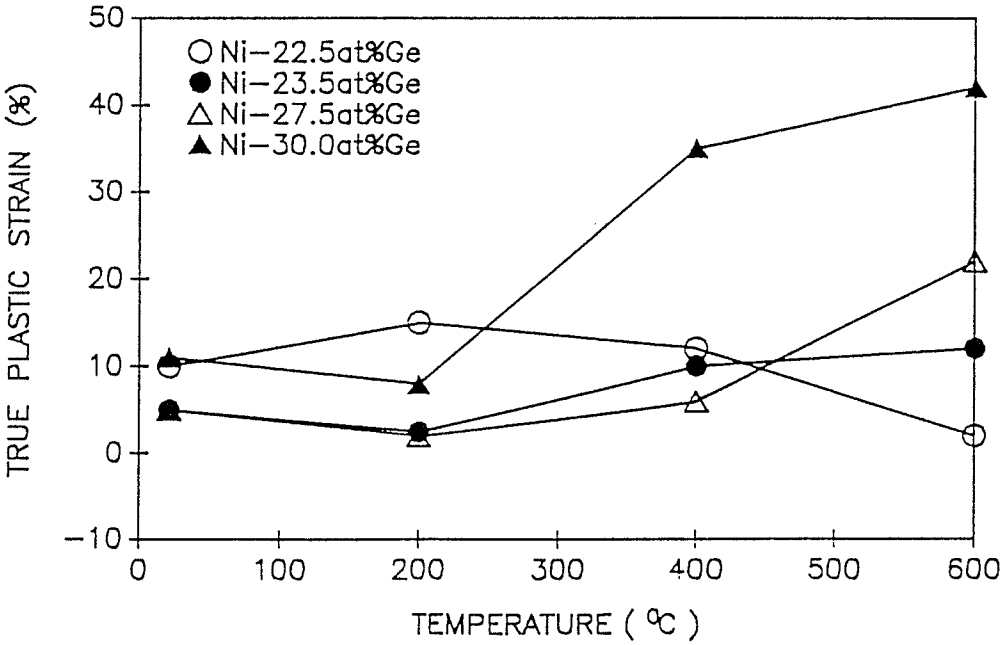

Fig 4.14 True plastic strain vs temperature for Ni-22.5at%Ge, Ni-23.5at%Ge, Ni-27.5at%Ge, and Ni-30.0at%Ge.

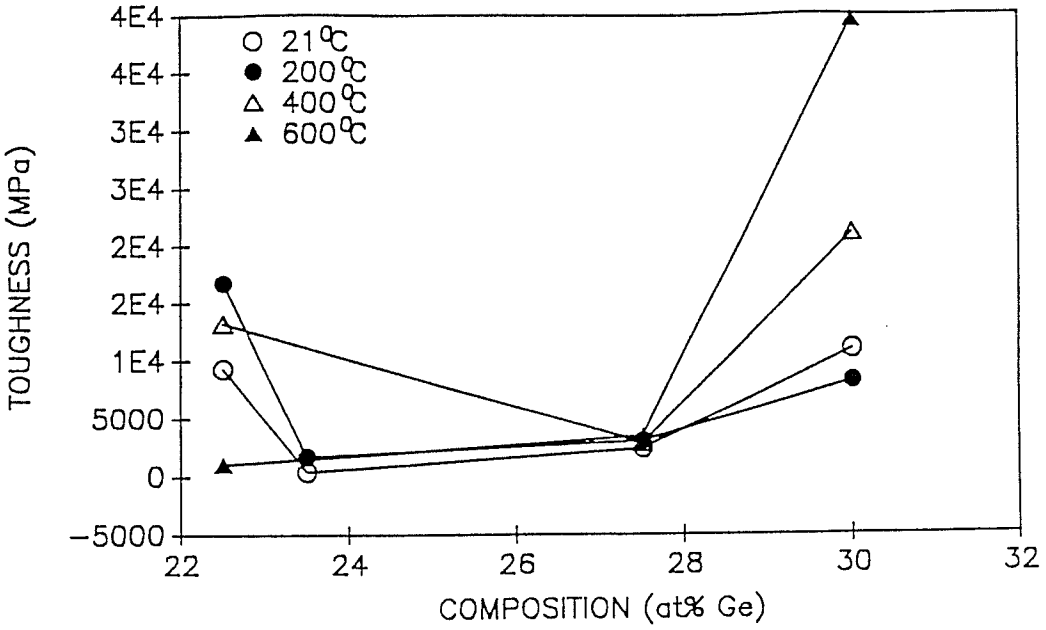

Fig 4.15 Toughness vs composition at 21°C, 200°C, 400°C, and 600°C.

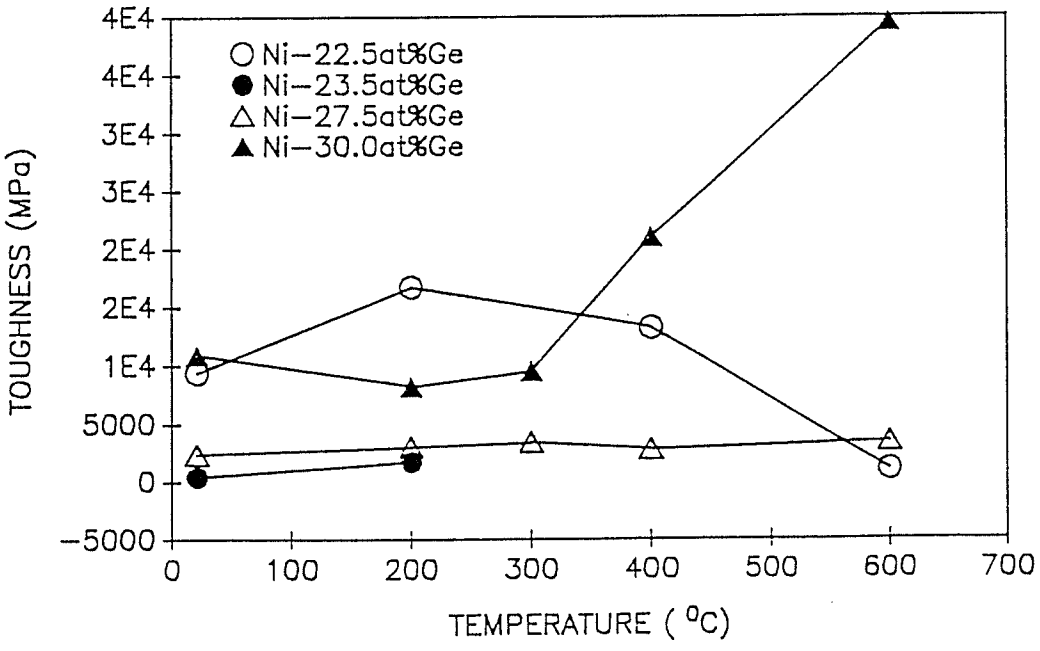

Fig 4.16 Toughness vs temperature for Ni-22.5at%Ge, Ni-23.5at%Ge, Ni-27.5at%Ge, and Ni-30.0at%Ge.

4.2.2 FRACTOGRAPHY

Some of the samples which were quite brittle broke before the 5000Kg load was applied and these samples were stored in a dessicator to avoid oxidation and later analysed on the SEM to identify the predominant mode of fracture. SEM offers a direct examination of the fracture surface without the need for preparation of thin films or surface replicas. It also has the advantage of greater depth of field. The secondary electron mode was used because it offers better resolution, produces an abundant signal and permits viewing of areas of the specimen that are not in a direct line of sight with the collector.

The identification of the direction of crack growth is extremely important in fractography and the location of the crack origin can help to identify the cause of failure.

Fracture characteristics vary depending on the microstructure as will be seen for samples examined in this study. The samples have been basically divided into two major fracture modes: ductile and brittle. Ductile fractures involve plastic deformation and appears dull and non-reflective to the naked eye. These fractures exhibit unique structures referred to as ductile dimples. Brittle fractures occur in components exhibiting little or no deformation i.e they fail in a nonplastic mode. They are further classified into intergranular and transgranular fractures. Intergranular fractures produces a rock-candy or faceted appearance whereas transgranular fractures propagate through the grains.

(a) Ni-22.5at%Ge:

This is a two phase material consisting of γ+γ'lamellae in γ' grains. Since grain boundaries are weak, the predominant mode is intergranular failure as we can see from fig 4.17. The grain facets show a rough and deformed appearance which is an indication that some shearing occurred before the boundaries failed. Most of the samples in this case did not break before 5000Kg load had been reached. The microstructures of these deformed samples will be discussed later.

(b) Ni-23.5at%Ge:

This structure consists of single phase γ'. Because of extremely low grain boundary cohesivity failure is intergranular at almost all temperatures. At lower temperatures (figs 4.18 to 4.22) sharp and clean grain facets are observed. Secondary cracks following the grain boundary can also be observed. But at temperatures 400°C and above (figs 4.23 to 4.27) some plastic deformation is evident within the grains although the failure mode is still largely intergranular. At higher magnifications we can see the individual grains separating out. At 584°C (figs 4.26 & 4.27) along with intergranular cracks some cleavage marks are also seen indicating a change in the mode of fracture.

(c) Ni-27.5at%Ge

This is a two phase material with a precipitation of Ni_5Ge_3 at the grain boundaries of Ni_3Ge. This precipitation brings some changes in the grain boundary cohesivity. At room temperature (figs 4.28 to 4.33) it can be observed that there are fewer grain

boundary cracks and that the two different phases exhibit different failure modes. One shows cleavage cracks and another shows clean and sharp grain facets. Cleavage cracks are present in Ni_5Ge_3 grains and intergranular in Ni_3Ge grains. This behavior reflects on the relative strength and hardness of the two phases. At still higher magnifications some cleavage steps are observed.

At 200°C (figs 4.34 to 4.36) it is observed that the mode of fracture is mainly cleavage/shearing and at very few places intergranular cracks can be observed. This implies that a fair amount of plasticity has set in at 200°C. At some places transgranular ceacks can be observed which are a further indication of improved ductility. At higher magnifications plate-like cleavage and river patterns are evident.

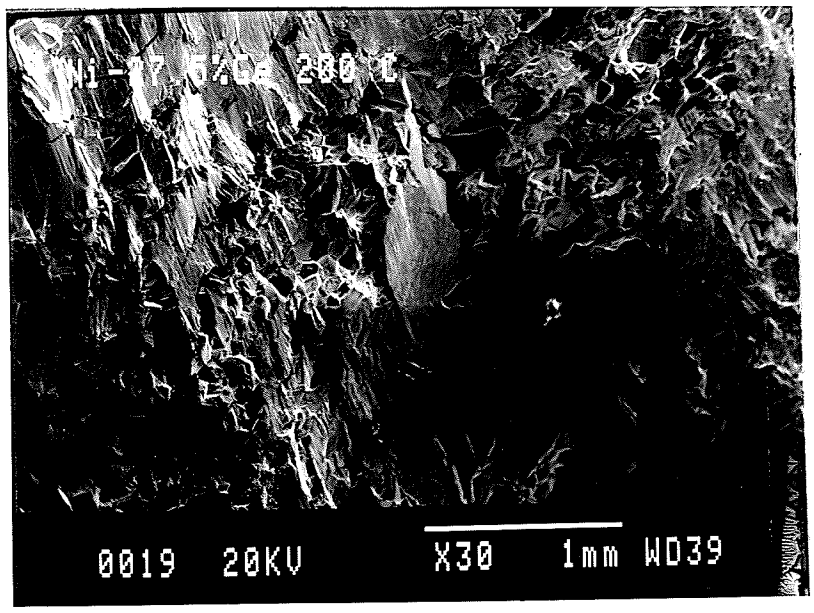

Fig 4.17 Ni-22.5 at% Ge failed at 200°C (30X)

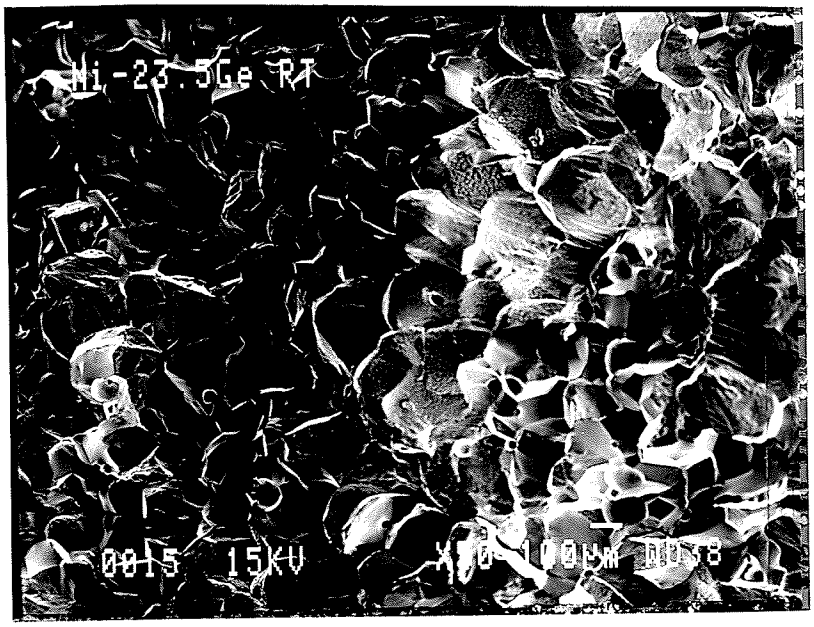

Fig 4.18 Ni-23.5 at % Ge failed at 21°C (50X)

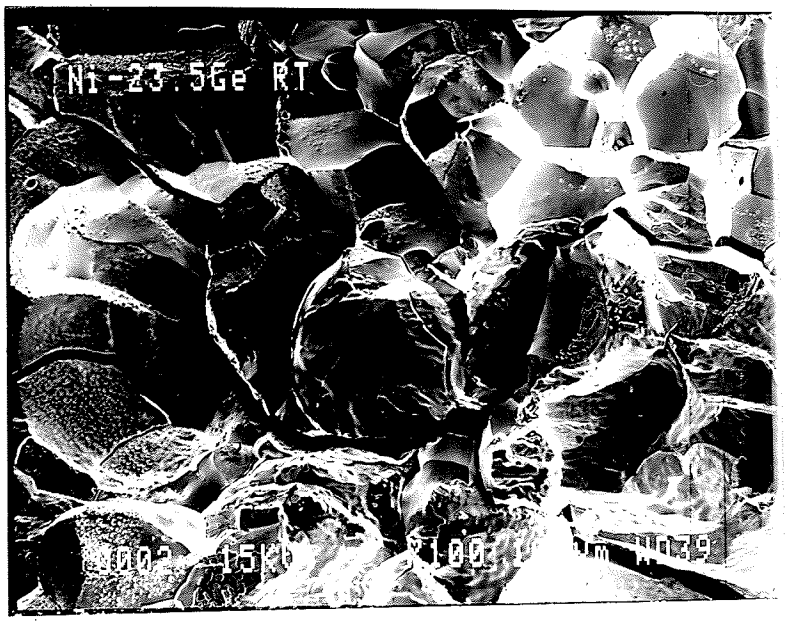

Fig 4.19 Ni-23.5 at % Ge failed at 21°C (100X)

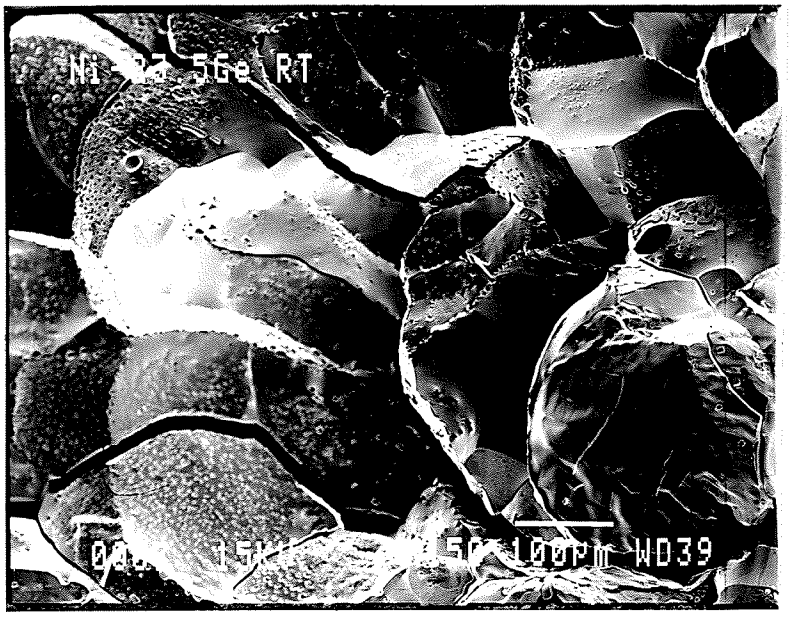

Fig 4.20 Ni-23.5 at% Ge failed at 21°C (150X)

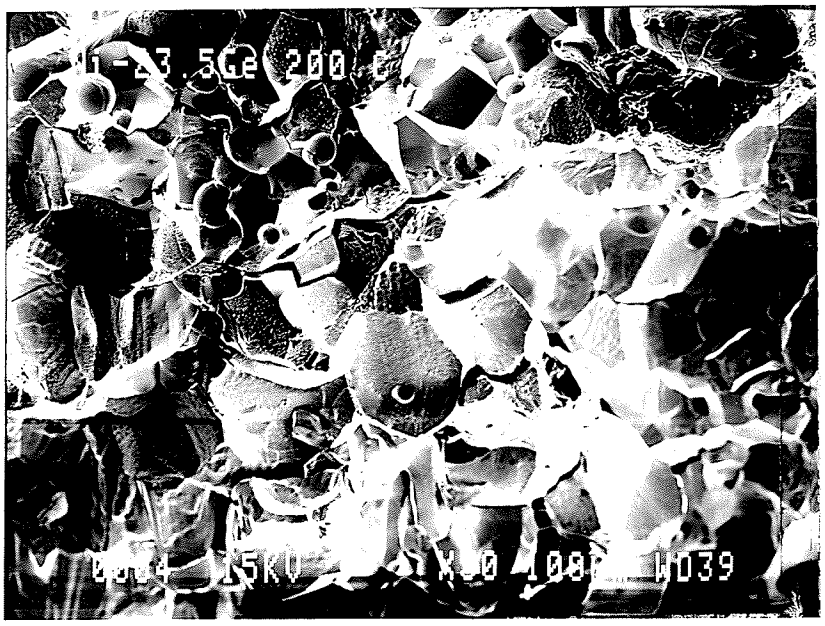

Fig 4.21 Ni-23.5 at% Ge failed at 200°C (50X)

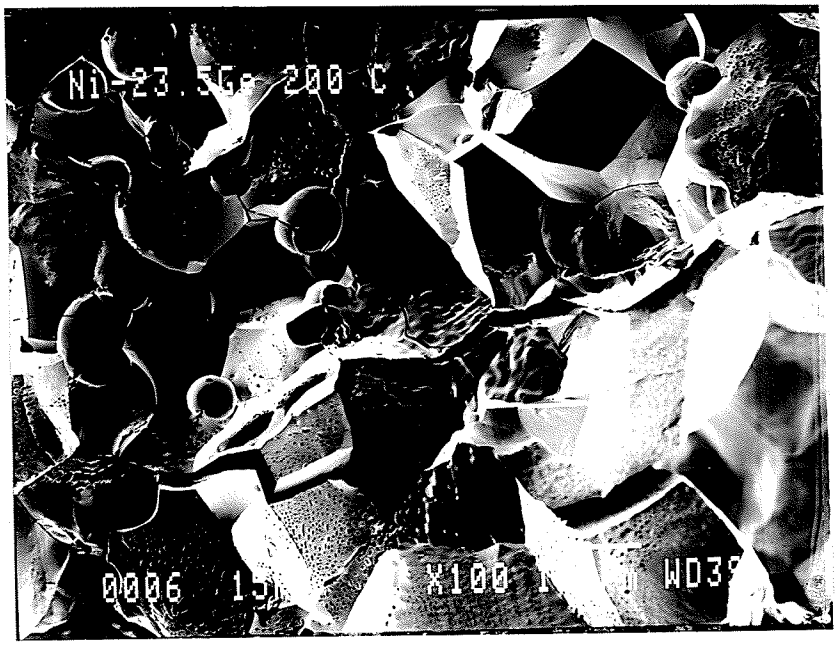

Fig 4.22 Ni-23.5 at% Ge failed at 200°C (100X)

Fig 4.23 Ni-23.5 at% Ge failed at 400°C (30X)

Fig 4.24 Ni-23.5 at% Ge failed at 400°C (60X)

Fig 4.25 Ni-23.5 at% Ge failed at 400°C (150X)

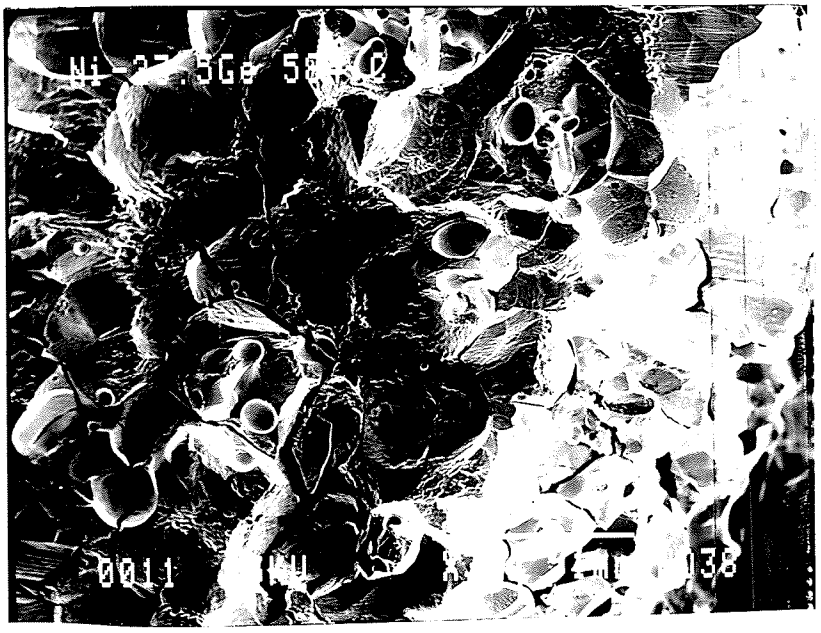

Fig 4.26 Ni-23.5 at% Ge failed at 584°C (30X)

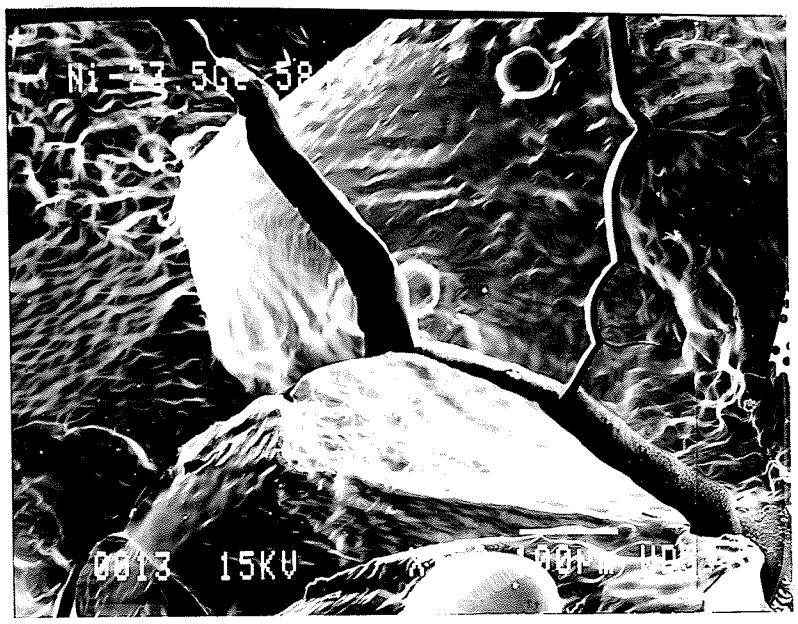

Fig 4.27 Ni-23.5 at% Ge failed at 584°C (150X)

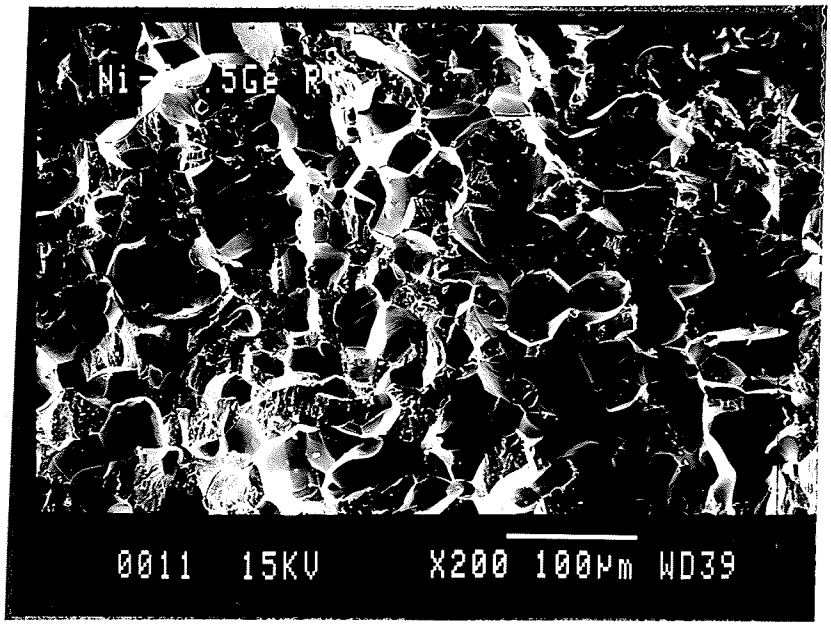

Fig 4.28 Ni-27.5 at% Ge failed at 21°C (200X)

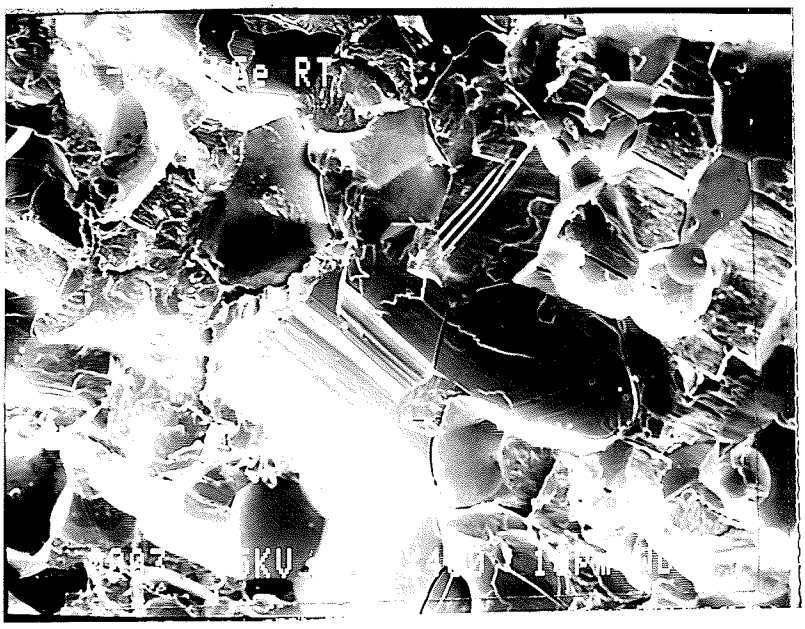

Fig 4.29 Ni-27.5 at% Ge failed at 21°C (400X)

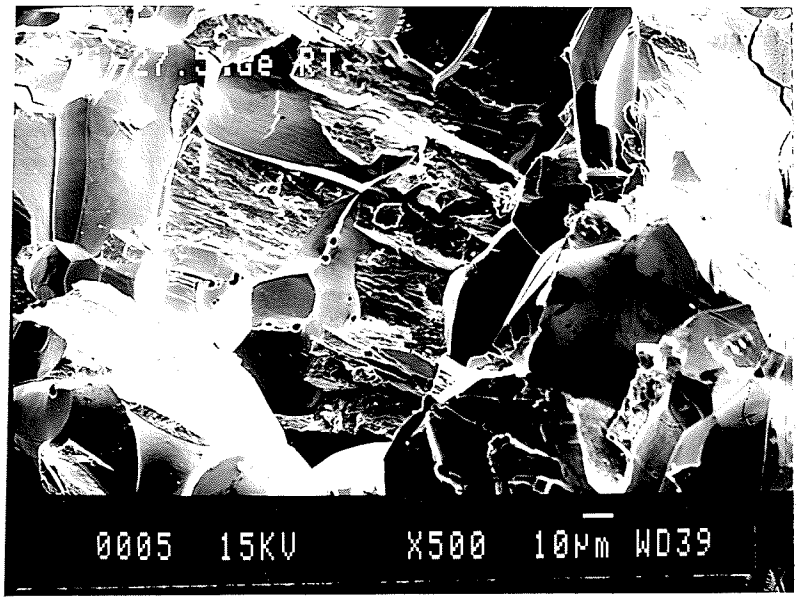

Fig 4.30 Ni-27.5 at% Ge failed at 21°C (500X)

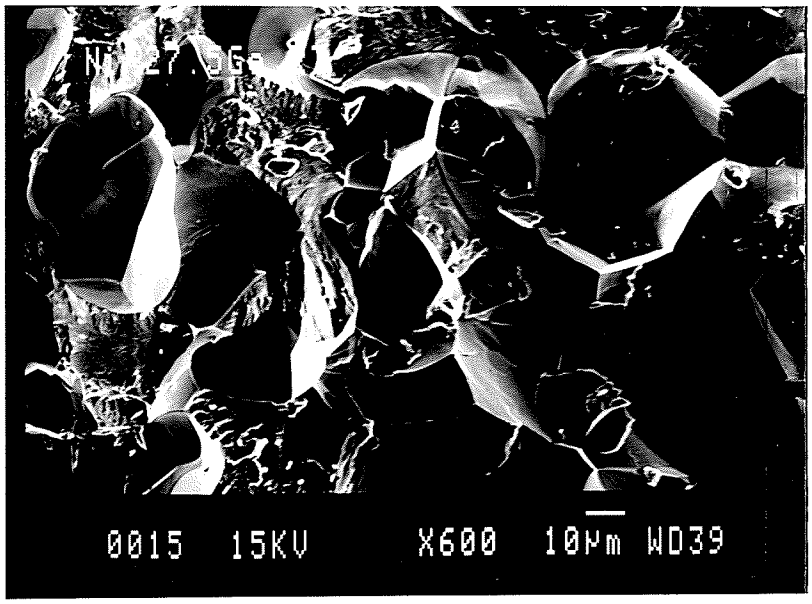

Fig 4.31 Ni-27.5 at% Ge failed at 21°C (600X)

Fig 4.32 Ni-27.5 at% Ge failed at 21°C (700X)

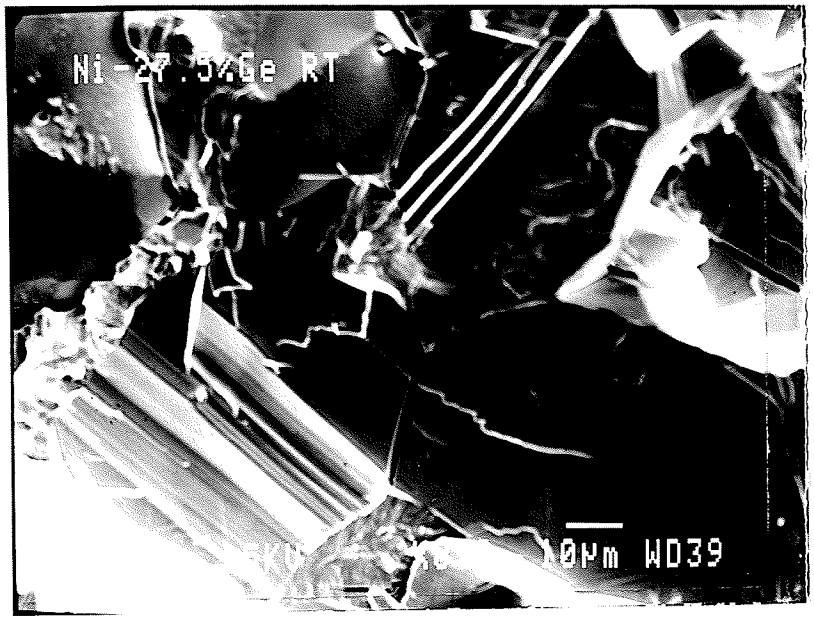

Fig 4.33 Ni-27.5 at% Ge failed at 21°C (850X)

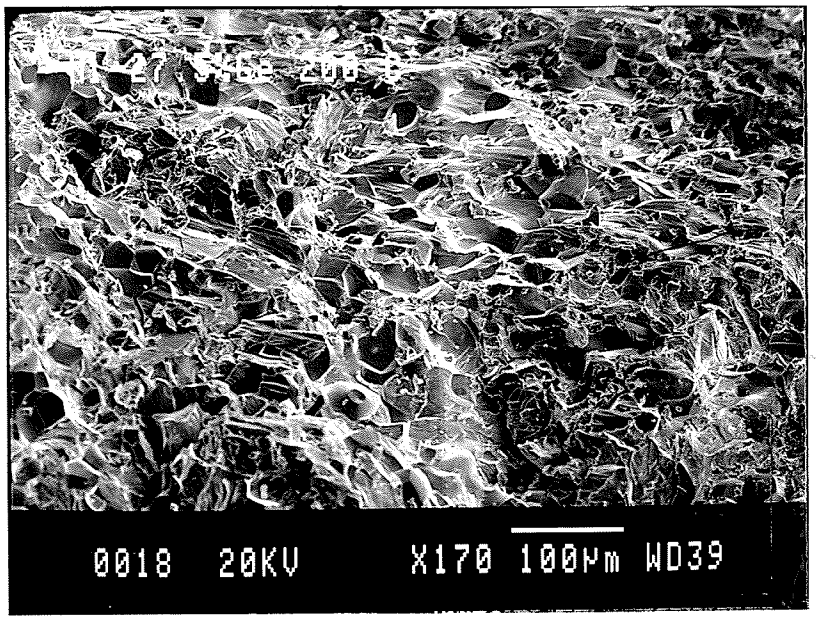

Fig 4.34 Ni-27.5 at% Ge failed at 200°C (170X)

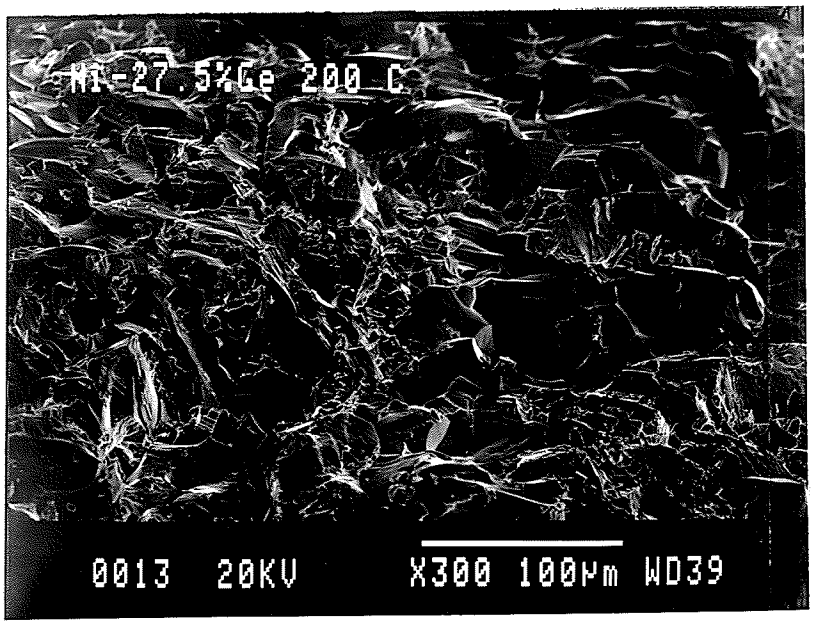

Fig 4.35 Ni-27.5 at% Ge failed at 200°C (300X)

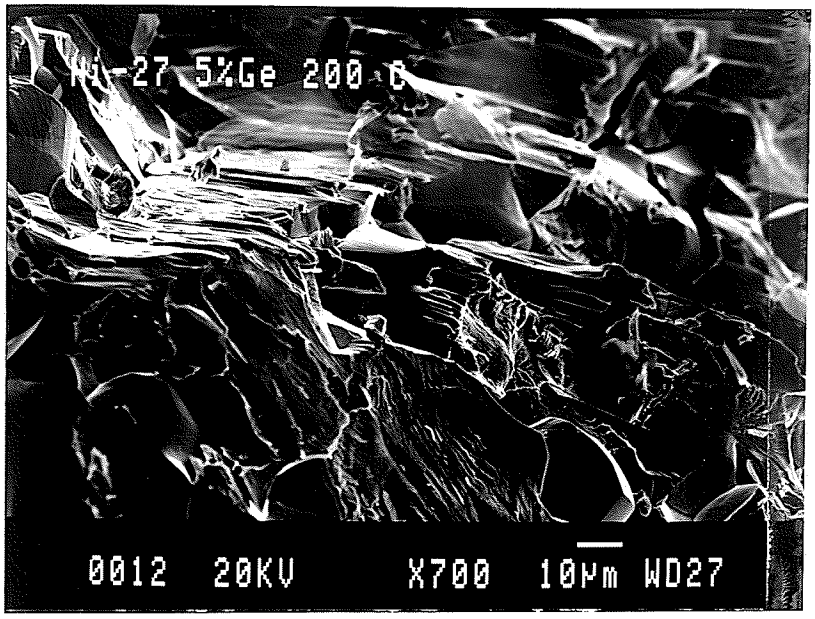

Fig 4.36 Ni-27.5 at% Ge failed at 200°C (700X)

4.2.3 OPTICAL METALLOGRAPHY OF DEFORMED SAMPLES AND MEASUREMENT OF MACROHARDNESS

Some of the samples which strain hardened and were less brittle just deformed and did not fail up to the maximum load. These were cut, mounted, polished, and etched. On observing the microstructures, cracks were seen which gave a clue as to their possible initiation site and predominant path of fracture.

Macrohardness results are listed in table 4.6. They show that the hardness values first increase with increasing temperature and then decrease. This shows that deformation at lower temperatures makes the material harder whereas softening overcomes the strain hardening at higher temperatures.

From the microstructures of the deformed samples we can infer the following:

Ni-22.5at%Ge: The samples show predominantly intergranular failure(figs 4.37 & 4.38) at all temperatures. This is because of lower grain boundary cohesivity of the Ni_3Ge grains. The cracks are seen to be continuous and wide.

Ni-25.0at%Ge: Single phase Ni_3Ge shows huge cracks along grain boundary (fig 4.39).

Ni-27.5at%Ge: In this specimena number of microcracks are visible. These cracks originate at the grain boundary and then propogate through the grains of Ni_5Ge_3 and also go along the grain boundaries at some places(fig 4.40). At higher temperatures(figs 4.41 & 4.42) it is seen that cracks also propagate across Ni_3Ge which is a positive sign of improved ductility.At 600°C(fig 4.43), the grains were deformed and the cracks were mostly present at the grain boundary.

Ni-30.0at%Ge: The cracking shows the same behavior as in Ni-27.5at%Ge. But in this

case the cracks are more diffuse and smaller in size(fig 4.45).Also, at higher temperatures the grains have deformed to a large extent(fig 4.46).

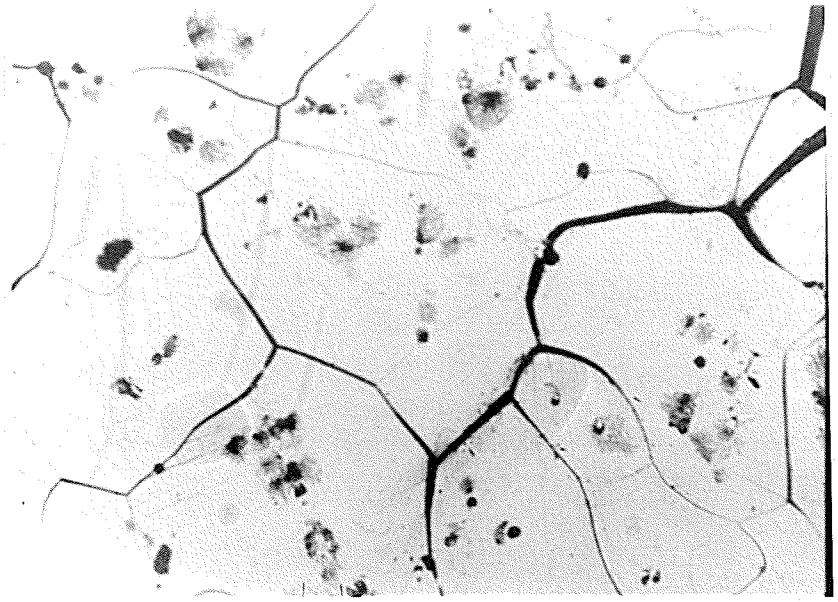

Fig 4.37 Ni-22.5 at% Ge deformed at 21°C (200X)

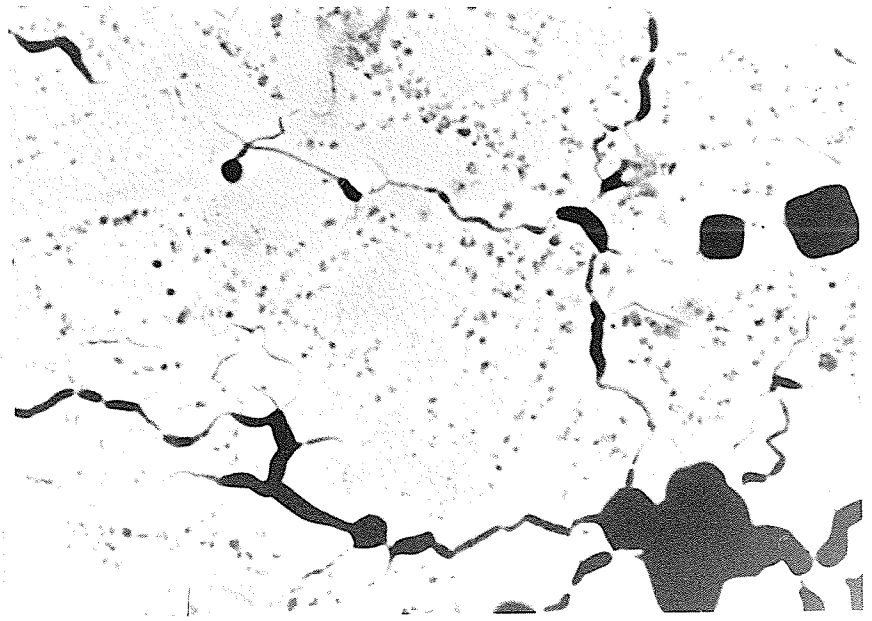

Fig 4.38 Ni-22.5 at% Ge deformed at 400°C (50X)

Fig 4.39 Ni-25.0 at% Ge deformed at 700°C (50X)

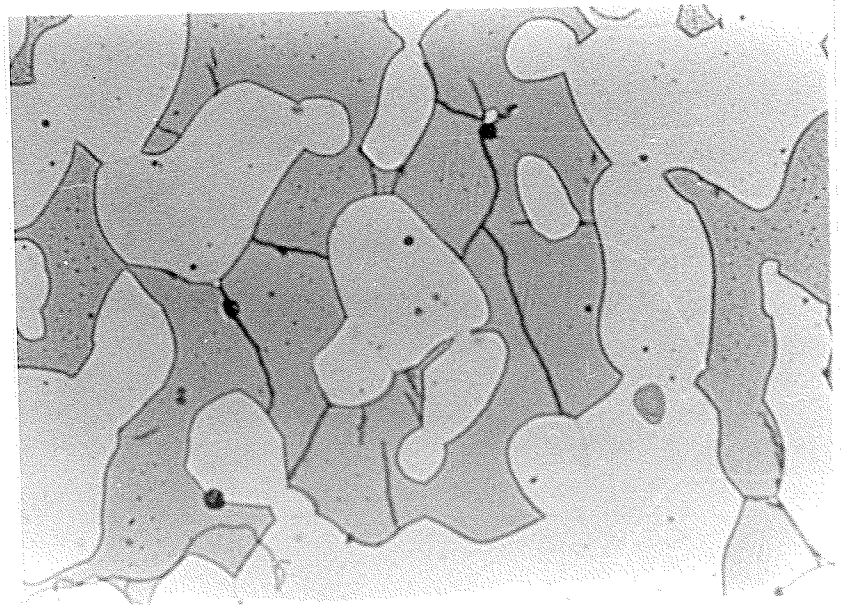

Fig 4.40 Ni-27.5 at% Ge deformed at 21°C (400X)

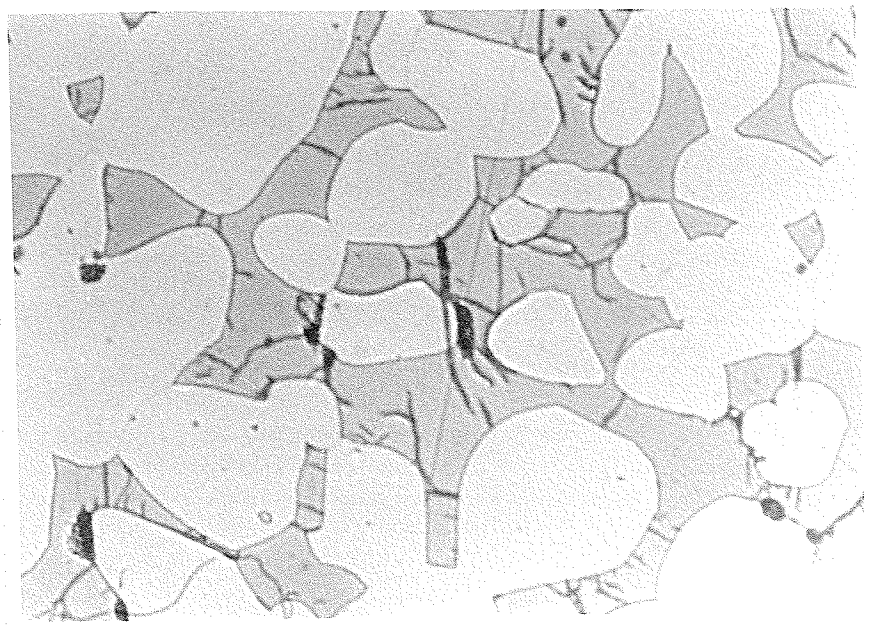

Fig 4.41 Ni-27.5 at% Ge deformed at 200°C (400X)

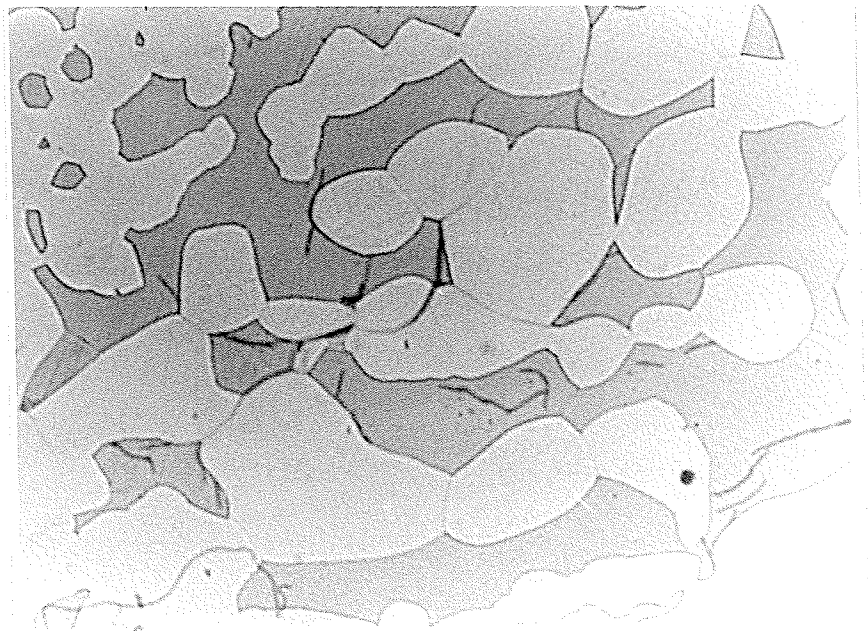

Fig 4.42 Ni-27.5 at% Ge deformed at 300°C (400X)

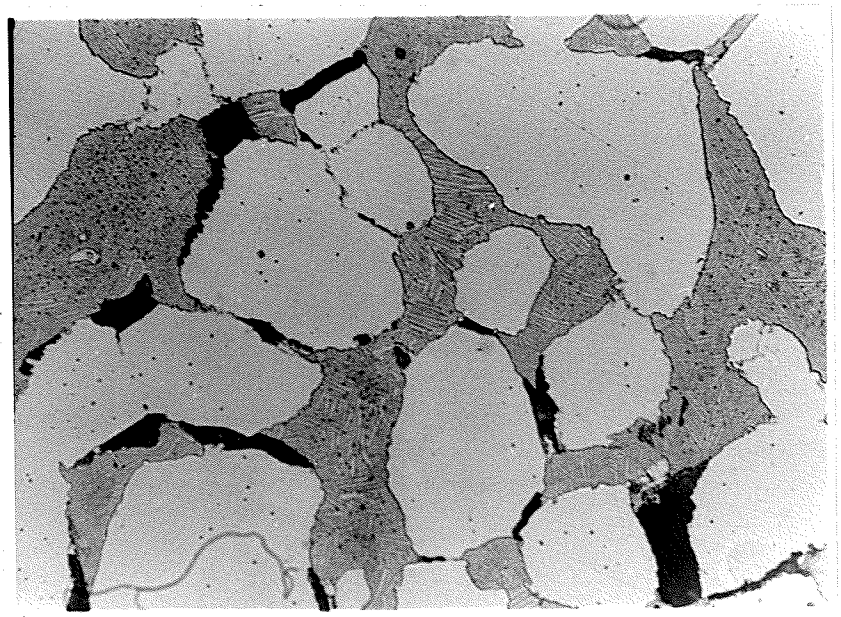

Fig 4.43 Ni-27.5 at% Ge deformed at 600°C (400X)

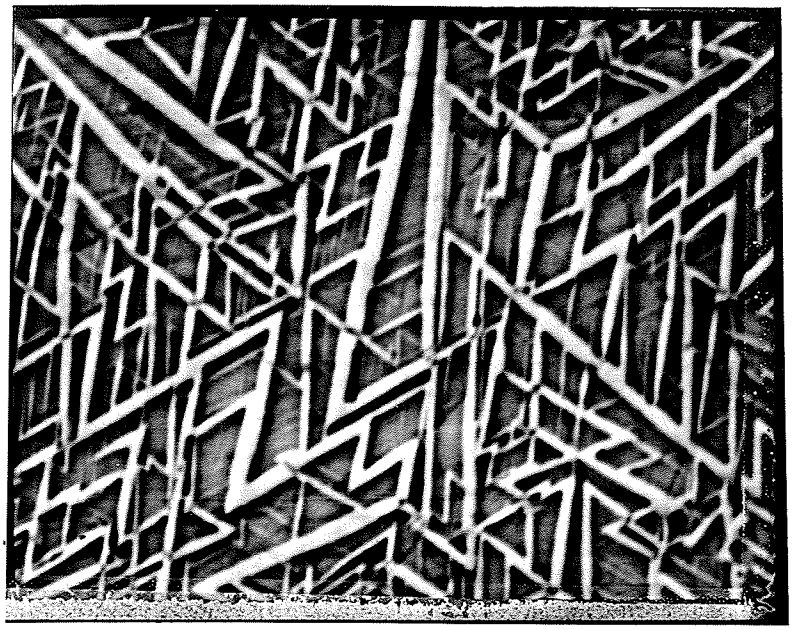

Fig 4.44 Ni-27.5 at% Ge deformed at 600°C (5000X)

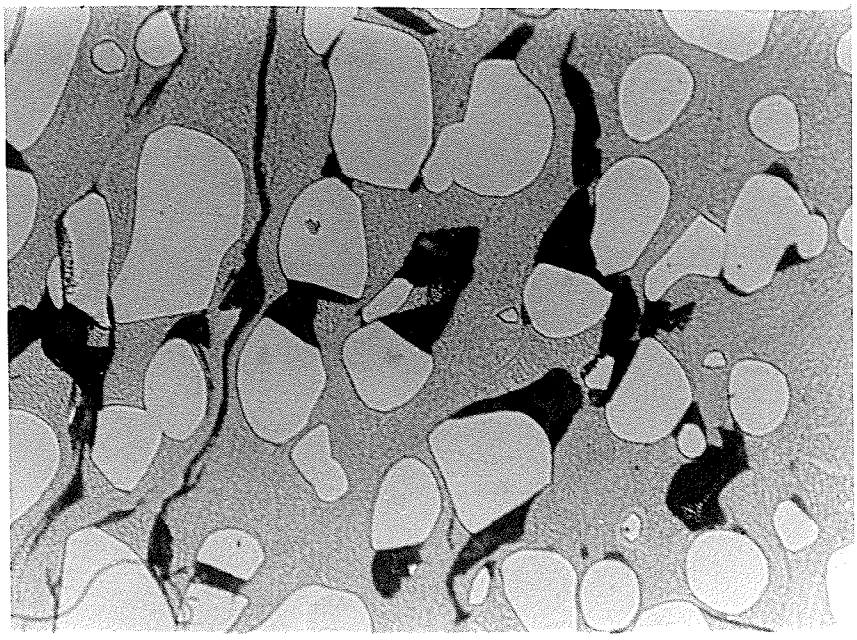

Fig 4.45 Ni-30.0 at% Ge deformed at 400°C (400X)

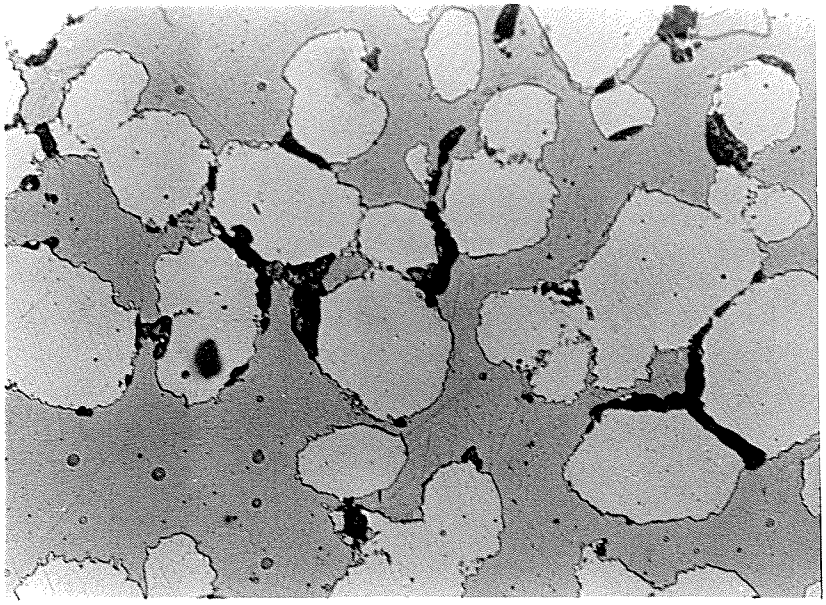

Fig 4.46 Ni-30.0 at% Ge deformed at 600°C (400X)

TABLE 4.6 : MACROHARDNESS MEASUREMENT OF THE DEFORMED SAMPLES(VHN)

Temperature	Ni-22.5%Ge	Ni-23.5%Ge	Ni-27.5%Ge	Ni-30.0%Ge
As Cast	327	317	612	724
homogenised	296	313	473	549
21°C	358	failed	487	540
200°C	386	failed	501	failed
400°C	353	failed	-	450
600°C	-	-	336	433

CHAPTER V

DISCUSSION

The characterisation of all six samples formed a backbone for interpreting the mechanical testing results. Three different phases were involved, solid solution of Ge in Ni, Ni_3Ge, and Ni_5Ge_3. Out of the three Ni_5Ge_3 has the largest value of microhardness.

After homogenising Ni-20.0at% Ge it still retains the dendritic structure. Extending the homogenising period did not bring any change. The possible reason might be the presence of disordered phase α along with the ordered phase Ni_3Ge, which might lower the diffusion rates. So may be by extending the homogenising time to a much larger degree might be able to improve the structure. Rapid solidification technique might be tried which gives much more homogenised structure than conventional casting.

A high degree of porosity was observed in some of the samples. In case of Ni-23.5at% Ge it was around 5%, which further enhanced the already low ductility of Ni_3Ge. This could have been avoided by proper processing technique.

Microstructure of the alloys showed the distribution of different phases which plays a critical role in determining the properties. In case of Ni-22.5at% Ge small regions of (α + Ni_3Ge) lamellae were present within the Ni_3Ge grains. Ni-23.5at%Ge consisted of equiaxed grains of Ni_3Ge. Except for the presence of (α + Ni_3Ge) lamellae the mechanical properties of the two alloys should be same. But these lamellae act as dislocation barrriers to slip motion thus giving higher strength compared to single phase Ni_3Ge. Ni-27.5at%Ge and Ni-30.0at%Ge showed precipitation of Ni_5Ge_3 at the grain

Ni_3Ge. Ni-27.5at%Ge and Ni-30.0at%Ge showed precipitation of Ni_5Ge_3 at the grain boundaries of Ni_3Ge. They were uniformly distributed and Ni-30.0at%Ge had a higher percentage of Ni_5Ge_3. The effect of Ni_5Ge_3 on the properties will be discussed later.

Compression tests were performed for two reasons. First, to see the effect of second phase on the strength and ductility of Ni_3Ge and second to see the effect of temperature on strength and ductility of the alloys.

Since the porosity level was quite high, so instead of emphasizing on the absolute values the discussion will be based mainly on comparison of the properties of the different alloys and how it can be related to the cracking behavior.

All the alloys showed anomalous behavior and since Ni_3Ge is present in all of them it might be the possible reason for this. Different reasons have been proposed to explain the anomalous behavior of $L1_2$ compounds. The one which is more emphasized is the cross-slip of screw dislocations from {111} plane to {100} plane(fig 5.1). Positive temperature dependence of the flow stress below T_p (peak strength temperature) is due to an anomalous increase in the critical resolved shear stress(CRSS) for {111}<110> slip with increasing temperature. Fall off in strength at temperatures above T_p is a direct consequence of the onset of another {100}<110> slip, which exhibits a normal temperature dependence. The {100}<110> slip is operative in place of the {111}<110> slip above T_p because the CRSS of the latter becomes higher than that of the former which reveals the positive temperature dependence.

The yield strength vs. temperature behavior showed that presence of α with Ni_3Ge increases the strength to a large extent and also increases the peak strength temperature.

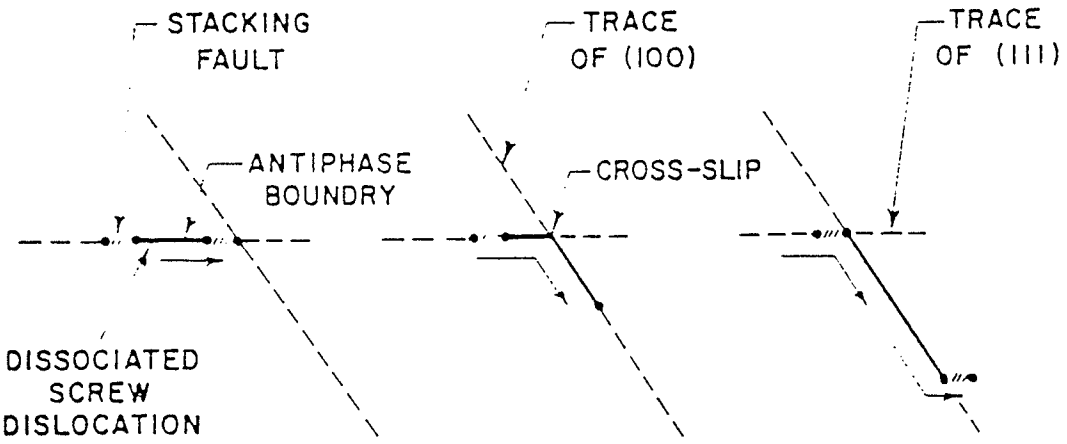

Fig 5.1 Cross-slip of a superlattice dislocation from the (111) slip plane into (100).(42)

Increase in peak strength temperature implies that cross-slip is occurring at higher temperatures which might be because of lamellar regions posing as dislocation barriers.

Ni_5Ge_3+Ni_3Ge containing alloy showed a slight increase in strength compared to Ni_3Ge but peak strength temperature was lowered. These results are quite consistent with the theories proposed which states that the grain boundary cohesivity depends on the valency difference between A and B. Therefore, increasing the A content leads to a positive valency difference thus increasing grain boundary cohesive strength whereas increasing B content leads to a negative valency difference thus decreasing grain boundary cohesive strength.

The temperature dependence of the deformation behavior showed that Ni-30at%Ge has the highest increase with temperature. Also according to Hall and Huang (7) the two phase structure is more deformable than single phase γ'. However, deformation of Ni-22.5at%Ge is limited because of a high strain hardening rate and the maximum occurs at a temperature of $\approx$ 200°C. Higher ductility of two phase alloys over that of single phase alloys indicates that microstructural features are important in determining the ductility.

In alloys containing γ+γ', the high temperature strength is borne mainly by the γ'-phase and the ductility is contributed by the primary solid solution of Ni. In the sense that the two materials contribute different properties, the alloys can be regarded as composite-like materials.

The strength of Ni_3Ge is higher compared to α+Ni_3Ge at 600°C. This implies that Ni_3Ge attains considerable plasticity at 600°C. This confirms Shashkovs proposal(45) that the transition from the brittle to plastic state occurs at temperatures around 550°C because

of the disappearance of directional atomic bonds. Also at high temperature, the ordered state is stronger than the disordered phase while at low temperatures when there is no diffusion taking place disordered material is stronger than ordered material. These were reflected in the results which showed that only at 600°C the %deformation goes up when we switch from (Ni)+Ni_3Ge to Ni_3Ge.

On proceeding from Ni_3Ge to Ni_3Ge+Ni_5Ge_3 there is an increase in deformation but the rate of increase with temperature is more pronounced as the temperature increases. This shows that the precipitation of Ni_5Ge_3 at the grain boundaries of Ni_3Ge increases the grain boundary cohesivity and leads to higher deformation rates.

For a better understanding of the observed behavior the failed and deformed samples were studied. Optical metallography of the deformed samples showed that in Ni-22.5 at% Ge since the precipitate is within the grains of Ni_3Ge, the failure is intergranular which is same as for pure Ni_3Ge. The only advantage of the second phase is that more stress is needed for the failure to occur because the lamellar regions pose as barriers to dislocation motion. For Ni-27.5 at% Ge and Ni-30.0 at% Ge the precipitation of second phase is at the grain boundary of Ni_3Ge and thus alters the grain boundary chemistry. It reduces the extent of intergranular failure and makes it more transgranular with cracks propagating mainly within the Ni_5Ge_3 grains. The cracks are diffuse and very fine. Thus crack morphology and distribution also affects the deformation behavior to a large extent. It has been proposed that diffuse cracks require more energy for complete failure. also, changing the cracking behavior from intergranular to transgranular improves ductility.

Fractography showed the completely brittle fracture in case of pure Ni_3Ge. But for

two phase Ni_5Ge_3 + Ni_3Ge the phases showed different failure modes. Ni_5Ge_3 failed by cleavage sort of fracture whereas Ni_3Ge showed shining grain facets implying brittle failure. In case of Ni-30.0at%Ge, where % of Ni_5Ge_3 is more the fracture is mostly cleavage and very few grain facets are seen. Similarly as one goes to higher temperatures the fracture behavior becomes mostly cleavage.

Toughness was found to be maximum for Ni-30.0 at% Ge and Ni-22.5 at% Ge. This value increased with temperature in the former case but it showed a peak for Ni-22.5at%Ge. Toughness did not vary with temperature in Ni-27.5 at% Ge.

Thus, from the results it can be said that out of all the compositions studied some are better in one respect and some in others so to acheive the best results an optimum composition has to be chosen and this requires extensive work.

CHAPTER VI

CONCLUSIONS

The conclusions of the present study are:

(1) It is difficult to homogenise a two phase material consisting of one ordered and one disordered phase.

(2) Microhardness of α is lower than that of Ni_3Ge which in turn is lower than Ni_5Ge_3. Thus α+Ni_3Ge has a lower hardness compared to Ni_3Ge whereas Ni_5Ge_3+Ni_3Ge has the highest hardness.

(3) The mechanical testing results confirm the anomalous behavior reported for Ni_3Ge. In all alloys where Ni_3Ge was one of the phases anomalous behavior was observed.

(4) α+Ni_3Ge showed a higher peak strength and peak strength temperature compared to Ni_3Ge and Ni_5Ge_3+Ni_3Ge did not have much improvement in peak strength over Ni_3Ge also it's peak strength temperature was lower.

(5) Comparing the results of Ni-27.5at%Ge and Ni-30.0at%Ge, it can be deduced that the volume fraction of the different phases affects the ductility. As the percentage of Ni_5Ge_3 increases ductility improves.

(6) In case of Ni-22.5at%Ge and Ni-23.5at%Ge the cracks are intergranular and continuous. In Ni-27.5at%Ge and Ni-30.0at%Ge presence of Ni_5Ge_3 at the grain boundaries of Ni_3Ge changes the crack morphology from continuous to diffuse and cracks are mostly transgranular branching out within Ni_5Ge_3 grains.

REFERENCES

(1) C.T.Sims and W.C.Hagel, "The Superalloys", John Wiley and Sons, 1967

(2) M.J.Donachie,Jr., "Superalloys-source book", ASM, 1984

(3) D.P.Pope, "High temperature ordered intermetallic alloys", Mat.res.soc.symp.proceedings, MRS, vol.81, 1987, pp3-11

(4) J.H.Westbrook, "Intermetallic compounds", John Wiley & Sons, 1967

(5) N.S.Stoloff and R.G.Davies, Progress in Mat.Sc., 13, 1966, pp3-84

(6) O.Izumi and T.Takasugi, "High Temp. Ordered Intermetallic alloys", Mat. Res. Soc. Symp. Proceedings, MRS, vol.81, 1987, pp173-182.

(7) S.C.Huang and E.L.Hall, submitted to Met. Trans.

(8) C.T.Liu, "High Temperature alloys: theory and design", Proc. of conference held in april, 1984, Maryland, edited by J.D.Steigler, published by M.S.AIME

(9) C.L.White and D.F.Stein, Metall.TransA, 9A, 1978, p13

(10) C.L.Briant and R.P.Messner, Phil.Mag., B-12, 1980, p569

(11) T.Takasugi and O.Izumi, Acta metall., 33, 1985, p1247

(12) K.Aoki, O.Izumi, J.Japan Inst. Met., 43, 1979, p1190

(13) C.T.Liu, C.L.White, and J.A.Horton, Acta Metall., 33, 1985, p213

(14) R.P.Messner and C.L.Briant, Acta metall., 30, 1982, p457

(15) E.M.Schulson, T.P.Weihs, I.Baker, H.J.Frost and J.A.Horton, Acta Metall., 34, 1986, p1395

(16) X.R.Quian and Y.T.Chou, Scr. Metall., 6, 1988, p157

(17) R.A.D.Mackenzie and S.L.Sass, Scr. Metall., 22, 1988, p1807

(18) H.Lee, "Effect of rapid solidification on microstructure and mechanical properties of Ni_3Al", Masters thesis, 1987,Inst.of metals, Shengyang, China.

(19) N.Masahashi, T.Takasugi, and O.Izumi, Acta Metall., 36, 1988, p1815

(20) S.Ochiai, Y.Mishima, M.Yodogawa, and T.Suzuki, Trans. Japan Inst.of metals, 27, 1986, p32

(21) Y.Mishima, S.Ochiai, M.Yodogawa, and T.Suzuki, Trans.Japan Inst.Metals, 27, 1986, p648

(22) Y.Mishima, S.Ochiai, N.Hamao, M.Yodogawa, and T.Suzuki, Trans. Japan Inst.Metals, 27, 1986, p648

(23) T.Takasugi and O.Izumi, Acta Metall., 33, 1985, pp1247-1258

(24) A.I.Taub, C.L.Briant, S.C.Huang, K.M.Chang, and M.R.Jackson,Scripta Metall., 20, 1986, pp129-134

(25) A.I.Taub and C.L.Briant, Acta Metall., 35, 1987,pp1597-1603

(26) D.M.Wee, O.Noguchi, Y.Oya, and T.Suzuki, Trans.JIM, 21, 1980, pp237-247

(27) N.S.Stoloff,Inter.Metals Review, vol.29,No.3, 1984, pp123-135

(28) S.J.Liang and D.P.Pope, Acta Metall.,25, 1977, pp485-493

(29) O.Noguchi, Y.Oya, and T.Suzuki, Met.Trans.A,12A,1981,pp1647-1653

(30) S.Ochiai, Y.Oya, and T.Suzuki, Acta Metall.,vol.32,No.2,1984,pp289-298

(31) C.L.Briant and A.I.Taub, Mat.Res.Soc.Symp.Proceedings,133,1989,p281

(32) M.E.Eberhart and D.D.Vvedensky, Scripta Metall.,22,1988,pp1183-1186

(33) D.M.Wee and T.Suzuki, Trans. JIM, 20,1979,pp634-646

(34) "Binary alloy phase diagrams" Handbook

(35) G.V.Samsonov and V.N.Bondarev, Germinides, Consultants Bureau(1969)

(36) T.Suzuki, Y.Oya, and S.Ochiai, Metall.Trans., 15A, 1984, p173

(37) T.Suzuki and Y.Oya, Acta Metall., 28, 1980, pp301-309

(38) H.Pak, T.Saburi, and S.Nenno, Trans. JIM, 18, 1977, pp617-626

(39) D.M.Wee and T.Suzuki, Trans.JIM, 20, 1979, p415

(40) T.Suzuki, Y.Oya, and D.M.Wee, Acta Metall., 28, 1980, p301

(41) S.Takeuchi, K.Suzuki, and M.Ichihara, Trans. JIM, 20, 1979, pp263-268

(42) B.H.Kear and H.G.F.Wilsdorf, Trans.Metall.Soc.AIME, 224,1962,p382.

(43) B.A.Grinberg et. al, Phys. Met. Metall., vol 46, No.4, pp117-139.

(44) K.Aoki and O.Izumi, Acta Metallurgica, 27, 1979, pp807-816.

(45) D.P.Shashkov, Izv.Akad.Nauk SSSR Metallurgy 4, 114(1968).